LINK PERFORMANCE ANALYSIS OF AN OPTICAL CDMA SYSTEM USING AN OPTICAL PREAMPLIFIER

by
PRABHAT KUMAR DUBEY

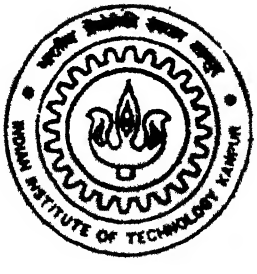

DEPARTMENT OF ELECTRICAL ENGINEERING
INDIAN INSTITUTE OF TECHNOLOGY KANPUR

January, 2000

LINK PERFORMANCE ANALYSIS OF AN OPTICAL CDMA SYSTEM USING AN OPTICAL PREAMPLIFIER

A Thesis submitted
In Partial Fulfillment of the Requirements

for the Degree of

MASTER OF TECHNOLOGY

By

PRABHAT KUMAR DUBEY

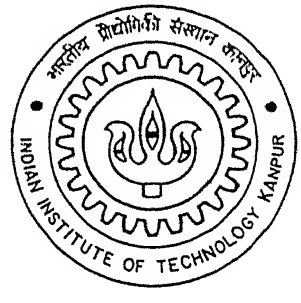

To the

DEPARTMENT OF ELECTRICAL ENGINEERING
INDIAN INSTITUTE OF TECHNOLOGY KANPUR

JANUARY, 2000

CERTIFICATE

This is to certify that the work contained in the thesis entitled **'LINK PERFORMANCE ANALYSIS OF AN OPTICAL CDMA SYSTEM USING AN OPTICAL PREAMPLIFIER'** *by* **PRABHAT KUMAR DUBEY** *has been carried out under my supervision and that this work has not been submitted elsewhere for a degree or diploma.*

Supervisor
Dr. P.K. CHATTERJEE
Professor
Department of Electrical Engineering
Indian Institute of Technology
Kanpur

January, 2000

DEDICATED TO

My Parents, who gave pre-emptive priority
to my studies bearing all troubles.

ABSTRACT

The spread spectrum code division multiple access (CDMA) allows asynchronous multiple access to a communication channel with no waiting time. The enormous bandwidth of optical fiber satisfies the high bandwidth requirement of CDMA. The electronic processing speed is a bottleneck for utilising the bandwidth of fiber, which can be overcome by the optical signal processing elements such as optical amplifiers and optical matched filters.

In this thesis we have studied optical CDMA (OCDMA) which is an extension of CDMA in optical domain. An optical preamplifier is placed after the optical matched filter in the receiver to increase the receiver sensitivity. A general optical orthogonal code (OOC) is used which has both crosscorrelation and autocorrelation bounded by unity. The optical intensity due to the interfering users correlated by the desired user's code at a particular user receiver is a random variable, and the Poisson count process of the detector further modifies its statistics to generate random current whose distribution is evaluated.

Thus, by analyzing a typical link in OCDMA system we have plotted the dependence of BER on the weight of OOC, number of users in the system, and input power per user to the receiver, for two different lengths of OOC. The nature of curves obtained is in agreement to the previous works.

These plots show that for users with data rate of 155Mbps an OCDMA system can be designed. The OOC with length 1024, weight 10, can be used in this system and 7 simultaneous users can be accommodated for BER<10^{-10}. If the length of code is increased to 4096, then we can accommodate 25 simultaneous users. The fiber span of this system, with optical preamplifier in receiver, is 100Kms. The increase in the fiber span is achieved without deterioration in performance of the system.

ACKNOWLEDGEMENT

I would like to express my sincere gratitude to my thesis supervisor Dr. P. K. Chatterjee for his help during my M.Tech thesis. Inspite of being busy, he was always available to help, guide and encourage me. His knowledge about my limitations, abilities, and interests made me work with my full efficiency. His faith and confidence in me acted as a catalyst for my work efficiency.

I would like to record my gratitude to Dr. A.K. Ghosh, Dr. R.K. Bansal, and Dr. S.K. Bose for their thought provoking instructions in various courses.

The goodwill and support of my friends Gaurav, Ashish and Kamlesh was also a great asset to me during my stay at IIT -Kanpur. I will be indebted to the help that Nitin gave me during the eleventh (sometimes twelfth too) hour of examinations.

Nothing would have been possible if the management of various facilities like Library, Computer Centre etc. was not proper. Thanks a lot to those who are there in backdrop to provide a congenial atmosphere.

Prabhat

CONTENTS

LIST OF FIGURES

LIST OF APPENDIX

CHAPTER 1

INTRODUCTION

The broadband communication requirements of the future generation will rely on optical fibers as the channel. The large bandwidth of optical fibers and very small propagation loss achieved through research in the field of material of fiber have made the optical systems an alternative for applications like video on demand, digital video, and multiplexing of various channels to form a high data rate channel as in SONET.

The field of digital communication has been using spread spectrum techniques since several years for accommodating multiple users in a single channel providing multiple access.

The bandwidth of spread spectrum signal is very large and this requirement is met by the enormous bandwidth of fiber. The scheme using spread spectrum technique in optical fiber communication is called optical code division multiple access (OCDMA).

1.1 CODE DIVISION MULTIPLE ACCESS

The classical multiple access schemes are: frequency division multiple access (FDMA), where one relies simply on separating the bands occupied by different users using different carriers for each of them; and a little harder to implement time division multiple access (TDMA) using different time slots for different users, where synchronization is the life blood for implementation. The relatively newer scheme called code division multiple access (CDMA) is based on spreading the spectrum of the user to an extent that the energy level reduces so much that it has flat, noise like characteristic. The spreading is done using pseudo noise (PN) sequence, which is pseudo random, and in addition various codes of a set possess property of quasi orthogonality. Hence signal of one user can be differentiated from that of the other, in spite of the fact that at all times and at all frequencies signals of all active users is present in the channel. The purpose of CDMA technique is enlisted as-

- Combating or suppressing the detrimental effect due to jamming, interference arising from other users of the channel, and self interference due to multi-path propagation.
- Hiding a signal by transmitting it at low power and, thus making it difficult for an unintended listener to detect it in the presence of background noise.
- Achieving message privacy in the presence of listeners.

1.2 OPTICAL CDMA

The optical analogue of FDMA namely WDMA was suggested for utilizing the enormous bandwidth of the fiber. The large bandwidth also logically led to the extension of CDMA systems from electrical to optical domain. The optical CDMA provides communication between transmitter and receiver pairs without synchronization. The following were the restrictions in development of OCDMA-

- The process of optical to electrical and electrical to optical conversion in a fiber optic based optical network for signal processing limits how much fiber bandwidth can be used because of limited speed of electronic processing.
- The PN sequences, Gold codes, and Hadamard Walsh sequences which are used for electronic CDMA cannot be used in OCDMA, as there is no concept of negative intensity of light- light adds incoherently except for very small aperture dimensions.

There is a continuous research going on to remove the first restriction: all-optical systems are now realized using components such as optical amplifier, optical multiplexer, and optical matched filter. The second restriction is overcome by development of optical orthogonal codes (OOC).

1.3 OPTICAL ORTHOGONAL CODES

The optical orthogonal codes are designed to achieve quasi-orthogonality between the members of a family of OOC. In contrast to the cancellation of positive and negative pulses used in electronic CDMA codes, these codes aim to minimize the interference between the shifted version of code with itself and also minimize interference between a code with shifted version of another code in the family. This is the reason why they are sparse in 1's.
The minimization conditions mentioned above could be mathematically expressed as auto and crosscorrelation constraints, and the number of 1's in the code is its weight. Several algebraic techniques have been proposed to meet these constraints.

1.4 BRIEF REVIEW ON OCDMA

The development of OOCs started when the concept of OCDMA was proposed. The implementation of these codes was made possible by the development of optical delay lines matched filter [12] and broad bandwidth fibers. The experimental set-up was first done by Prucnal et al [11] in which they observed the BER of system using Gold codes and Prime codes. The field of OCDMA got a boost when J.A. Salehi published his widely known papers [1], [2]. This standardized the requirements of OCDMA system and codes. He also provided bounds for the crosscorrelation values of OOCs using general codes,

which in turn provided bound for BER of systems using these codes. A detailed design, analysis and application of OOCs is given in [4]. The system using quasi-prime code is described in [6].
Ultra short pulse CDMA system scheme has been proposed in and the set-up is also given for realizing it [3]. In this work coding is done in frequency domain.

In all these works OCDMA systems have been designed for local area networks. As there is no provision for optical amplifier (or repeaters) in these, so they have geographical range limitation.

1.5 PROBLEM FORMULATION

In the present work, we have tried to increase the fiber span between two star couplers in a typical optical CDMA system shown in Figure 2.2.1, or in other words tried to increase the receiver sensitivity. For this a preamplifier is required because the signal level falls as the fiber span is increased, due to added attenuation. There are three options to achieve the increase in receiver sensitivity. We can use an APD detector instead of PIN diode, but the limited bandwidth of APD (< 1GHz) imposes restriction on its use in amplifying OCDMA signal. The other option is in-line electrical signal amplifier, but the problem of conversion from optical to electrical and then back, in addition to decoding and coding CDMA signal, is faced. This can be avoided by introducing a photonic preamplifier like EDFA. The broad bandwidth of EDFA (section 3.2) suits the need of high bandwidth OCDMA signal.

The photonic preamplifier in an OCDMA receiver, (Figure 2.2.1), can be placed either before the matched filter, amplifying the signal from all other users, or after the matched filter, amplifying the auto and crosscorrelation outputs. We have placed the amplifier after the matched filter because by this choice we end up amplifying only the small crosscorrelation peaks of the other users. The desired signal gives high autocorrelation peak, which is amplified to get high power desired bit signal.

The determination of the probability density function of the interfering user signals at the receiver of a particular user is cumbersome, so we have not determined it exactly, but the bounds suggested in [2] are taken for simplicity. The users in the system are large in number and are independent, identically distributed random variables, so central limit theorem can be invoked helping in reducing the mathematical complexity.

The count process in photo detection has a Poisson distribution, which modifies the input optical intensity statistics to yield a different optical current distribution. We have calculated the distribution of photo detector current for the random input optical intensity. For this we have used short time counting approximation to handle the count process.

By analyzing a typical OCDMA link, we have found out the bit error rate performance and its dependence on the optical orthogonal code parameters: length of the code and the weight of code. We have used a general OOC for this purpose, which has both auto and

crosscorrelation bounded by unity, (section 2.1.1). The dependence of BER on input power is also evaluated and plotted.

1.6 THESIS LAYOUT

In chapter 2, we have reviewed OCDMA systems in detail with emphasis on optical orthogonal codes-properties and requirements-and previous work done in optical CDMA field.

In chapter 3, the components of a typical optical CDMA link have been discussed with their specifications and principles in brief.

In chapter 4, we have done the performance analysis of general CDMA code used in a OCDMA link .We have considered the receiver of a particular user with optical preamplifier and evaluated the desired signal power, the interferer noise power and other noises in a optical system.

In chapter 5, we have plotted and discussed the BER expression obtained in the previous chapter, taking the various parameters as variables.

In chapter 6, we conclude our work pointing out the effect of the various parameters on the performance of OCDMA system and suggesting the value of parameters for which system works satisfactorily.

CHAPTER 2

REVIEW ON OPTICAL CDMA

In this chapter we will be discussing the properties of optical orthogonal codes and a bound on the number of codes which can be constructed from a given length and weight, along with the autocorrelation and crosscorrelation constraints on them. Also we will discuss the work which has been done in the field of optical CDMA (OCDMA) systems using various optical orthogonal codes (OOC).

2.1 OPTICAL ORTHOGONAL CODES

An optical orthogonal code is a family of (0,1) sequences with good auto and crosscorrelation properties. The code (also referred to as signature sequence) should be designed such that the autocorrelation is a peak and crosscorrelation are low throughout. This property is key to extracting signature sequence in presence of other user's signature sequence at the receiver end of a user. Therefore a set of signature sequences that are distinguishable from time shifted version of themselves and further two such signature sequences easily distinguishable from each other, is needed.

2.1.1 FUNDAMENTAL PROPERTIES OF OOCS

Let us consider a $(F,K,\lambda_a,\lambda_c)$ OOC set where

F– length of code
K- weight of code (number of ones in code)
λ_a- upper bound on autocorrealation values of sequences in the code
λ_c- upper bound on crosscorrelation values of the sequences in the code

Consider two periodic signals x(t) and y(t) written as

$$x(t) = \frac{1}{T_c} \sum_{n=-\infty}^{n=\infty} x_n P_{T_c}(t - nT_c)$$

where P_{T_c} is a rectangular pulse of duration T_c

$$x(t+T) = x(t), \text{ and}$$

$$y(t) = \frac{1}{T_c} \sum_{n=-\infty}^{n=\infty} y_n P_{T_c}(t - nT_c)$$

$$y(t+T) = y(t)$$

Let $X=(x_n)$ and $Y=(y_n)$ be two particular codes of an OOC family 'C' having period $F=T/T_c$

For some value of τ such that $0 \leq \tau \leq T$, and some l, where l is an integer $0 \leq l \leq F-1$ we can express the properties of OOCs as follows

- The condition on autocorrelation function is

$$\sum_{n=0}^{F-1} x_n x_{n+l} \begin{cases} \leq K for l = 0 \\ \leq \lambda_a for 1 \leq l \leq (F-1) \end{cases}$$

- The condition on crosscorrelation function can be expressed in the form of each pair of sequences X and Y such that $X \neq Y$

$$\sum_{n=0}^{F-1} x_n y_{n+l} \leq \lambda_c for 0 \leq l \leq (F-1)$$

K, λ_a, λ_c are constants which parameterize the OOC family.
Here note that strict orthogonality will require $\lambda_a=\lambda_c=0$. But in our case, sequence is defined to be orthogonal with respect to its shifted version if λ_a takes its minimal value, and two sequences are said to be orthogonal if λ_c takes on its minimal value.

In positive systems like optical systems (because there is incoherent addition of signals resulting in non-negative power of light) $x_n, y_n \in \{0,1\}$

An example of two codes from a class 'C' of family of optical orthogonal codes with parameter (32,4,1,1) is given in Figure 2.1. These codes can be represented as OOC s. Code A has ones at 1st, 10th, 13th,and 28th chip position while code B has ones at 1st, 5th, 12th,and 31st chip positions. The fundamental rule that ensures OOC's A and B to have periodic autocorrelation peak (K) and low periodic correlation ($\leq \lambda_a$) at any other shifts, with T_c as the unit of time shift, can best be explained from a simple set theory. The codes A and B are represented by equivalent set –

$$A=\{\tau_1^A, \tau_2^A, \tau_3^A, \tau_4^A\} \quad (2.1.1)$$

$$B=\{\tau_1^B, \tau_2^B, \tau_3^B, \tau_4^B\} \quad (2.1.2)$$

where τ_1^A=the relative delay between the beginning of the fist pulse and second pulse and so on...Similarly τ_1^B is the relative delay between the beginning of the fist pulse and second pulse and so on...

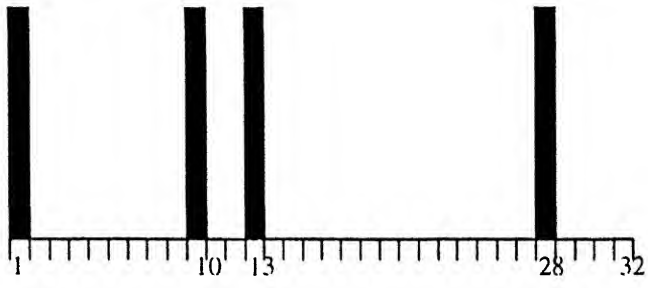

CODE A

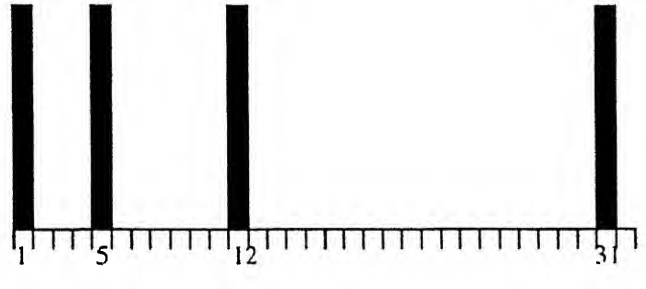

CODE B

Figure 2.1 The two optical orthogonal codes with bars depicting positions of pulses

An extended set of set A, A_{EXT}, with all linear combinations of jointly connected delays of different lengths is constructed by the following rule:

- Step1: Let the first four, i.e. K, delay elements of the set A_{EXT} be the delay elements of set A in Eqn.(2.1.1) i.e. $\tau_1^A, \tau_2^A, \tau_3^A, \tau_4^A$
- Step2: Let the next four, i.e.K, delay elements of the set A_{EXT} be the sum of all connected elements of size two, i.e. $\tau_1^A+\tau_2^A, \tau_2^A+\tau_3^A, \tau_3^A+\tau_4^A, \tau_4^A+\tau_1^A$ for periodic sequence A.

Note that $\tau_1^A+\tau_3^A$, $\tau_2^A+\tau_4^A$ are not the elements of set A_{EXT} as they are disjoint delay elements and cannot occur independently.

- Step (K-1): Let the (K-1)th (3^{rd} for this example) group of K delay elements of the set A_{EXT} be the sum of all connected delay elements of size (K-1) (3 for this example) i.e., $\tau_1^A+\tau_2^A+\tau_3^A, \tau_2^A+\tau_3^A+\tau_4^A, \tau_3^A+\tau_4^A+\tau_1^A, \tau_4^A+\tau_1^A+\tau_2^A$ for periodic sequence A.

The delay elements of size four (K), $\tau_1^A+\tau_2^A+\tau_3^A+\tau_4^A=T$ is not an element of set A_{EXT}, so A_{EXT} can be written as

$$A_{EXT}=\{\tau_1^A,\tau_2^A,\tau_3^A,\tau_4^A,\tau_1^A+\tau_2^A,\tau_2^A+\tau_3^A,\tau_3^A+\tau_4^A,\tau_4^A+\tau_1,\tau_1^A+\tau_2^A+\tau_3^A,\tau_2^A+\tau_3^A+\tau_4^A,$$
$$\tau_3^A+\tau_4^A+\tau_1^A,\tau_4^A+\tau_1^A+\tau_2^A\}$$

Total number of elements in $A_{EXT}=|A_{EXT}|=12$.

$$B_{EXT}=\{\tau_1^B,\tau_2^B,\tau_3^B,\tau_4^B,\tau_1^B+\tau_2^B,\tau_2^B+\tau_3^B,\tau_3^B+\tau_4^B,\tau_4^B+\tau_1^B,\tau_1^B+\tau_2^B+\tau_3^B,\tau_2^B+\tau_3^B+\tau_4^B,$$
$$\tau_3^A+\tau_4^B+\tau_1^B,\tau_4^B+\tau_1^B+\tau_2^B\}$$

In general for (F, K, 1,1) OOC, the construction of its extended set has (K-1) steps with K elements in each step. So the total number of elements in the extended set of an OOC, with $\lambda_a=\lambda_c=1$ is K(K-1).

For the sequence or code A to satisfy periodic autocorrelation property with $\lambda_a=1$, there should be non-repeated delay elements in the set A_{EXT}.

We require for two sequences A and B in addition to autocorrelation property, the crosscorrelation property to be satisfied. So for $\lambda_c=1$, the time delay elements in A and B should be non-repetitive i.e.

$$A_{EXT}\cap B_{EXT}=\phi \qquad ,\phi \text{ is a null set.}$$

In general for a given integer code length F and weight K where $K(K-1)\le F-1$ and $\lambda_a=\lambda_c=1$, one can construct at most N OOCs, A^i, such that there corresponding extended sets A^i_{EXT} for $1\le i\le N$, have no repeated elements and,

$$|A^i_{EXT}|=K(K-1) \qquad (2.1.3)$$
$$A^i_{EXT}\cap B^j_{EXT}=\phi \qquad (2.1.4)$$

for all $1\le i,j\le N$

From (2.1.3) and (2.1.4) we have $|C|$, the cardinality of OOC family 'C', is constrained as

$$|C|\le\lfloor (F-1)/K(K-1)\rfloor \quad , \text{ where}\lfloor\ \rfloor \text{ represents floor function} \qquad (2.1.5)$$

Thus OOCs achieve quasi orthogonality by avoiding coincidences in two codes vis a vis cancellation in Walsh-Hadamard codes used in electronic CDMA.

2.1.2 CONSTRUCTION ON OPTICAL ORTHOGONAL CODES

Various techniques are proposed for construction of OOCs like prime codes, quasi-prime codes, quadratic congruence codes, combinatorial methods, and projective geometry codes. Out of these the projective geometry codes are found to be most suitable.

The problem with the prime codes, quasi-prime codes, and quadratic congruence codes is that the number of code words becomes very small compared to the length of the code as the latter increases. Therefore, even to have a moderate number of users in the optical CDMA system, we will have to use a very high chip rate. The projective geometry codes achieve optimal codes for large number of code words.

The crosscorrelation is independent of code length for prime code. For the quadratic congruence code the auto and crosscorrelation constraints do not depend on the code length. This means that as the code length increases, or in other words as the autocorrelation peak increases, the crosscorrelation peak remains at a constant level. It results in a better detection performance. As can be seen from Table 2.1.1 the prime codes and quasi-prime codes do not appear to be suitable for applications in CDMA networks. Here the quadratic convergence codes can prove to be useful.

Code parameter	Prime code	Quasi prime code	Quad. Cong. Code	Projective geometry code PG(m,q)
Code length(F)	K^2	$(p-1)K^2<rK<pK^2$ $p\in I$	K^2	$(q^{m+1}-1)/(q-1)$
Code weight(K)	K	R	K	$(q^{s+1}-1)/(q-1)$
λ_a	K-1	(K-1)p	2	$(q^s-1)/(q-1)$
λ_c	2	2p	4	$(q^s-1)/(q-1)$
Cardinality | C |	K	K	K-1	$\lfloor(nCs+1/wCs+1\rfloor$
Optimality	Far from optimal	Far from optimal	Far from optimal	Optimal for even m=s=1

Table 2.1.1 Comparison of $(F,K,\lambda_a,\lambda_c)$ OOC [5]

2.2 DETAILED REVIEW OF OPTICAL CDMA

The enormous bandwidth of fiber which can be efficiently used for broad band optical CDMA signals (in direct sequence modulation) provided a motivation to use the plane old electronic CDMA in optical domain. The availability of optical encoders in form of optical tapped delay line (to be discussed in detail in next chapter) and decoder using an optical matched filter gave ground to experiment the OOCs in OCDMA systems. For a typical scheme of OCDMA system see Figure 2.2.1.A typical FO-CDMA system is best represented by an information (data) source, followed by a laser, when the information is in electrical signal form. The optical encoder maps each bit of the output information into a very high rate optical sequence which is coupled to a single mode fiber channel. At the receiver end of OCDMA the optical sequence is compared to stored self-replica of itself (correlation process) and to a threshold level at the comparator for data recovery.

Utilizing various optical orthogonal codes several experimental results have been reported from time to time, we will discuss them here briefly.

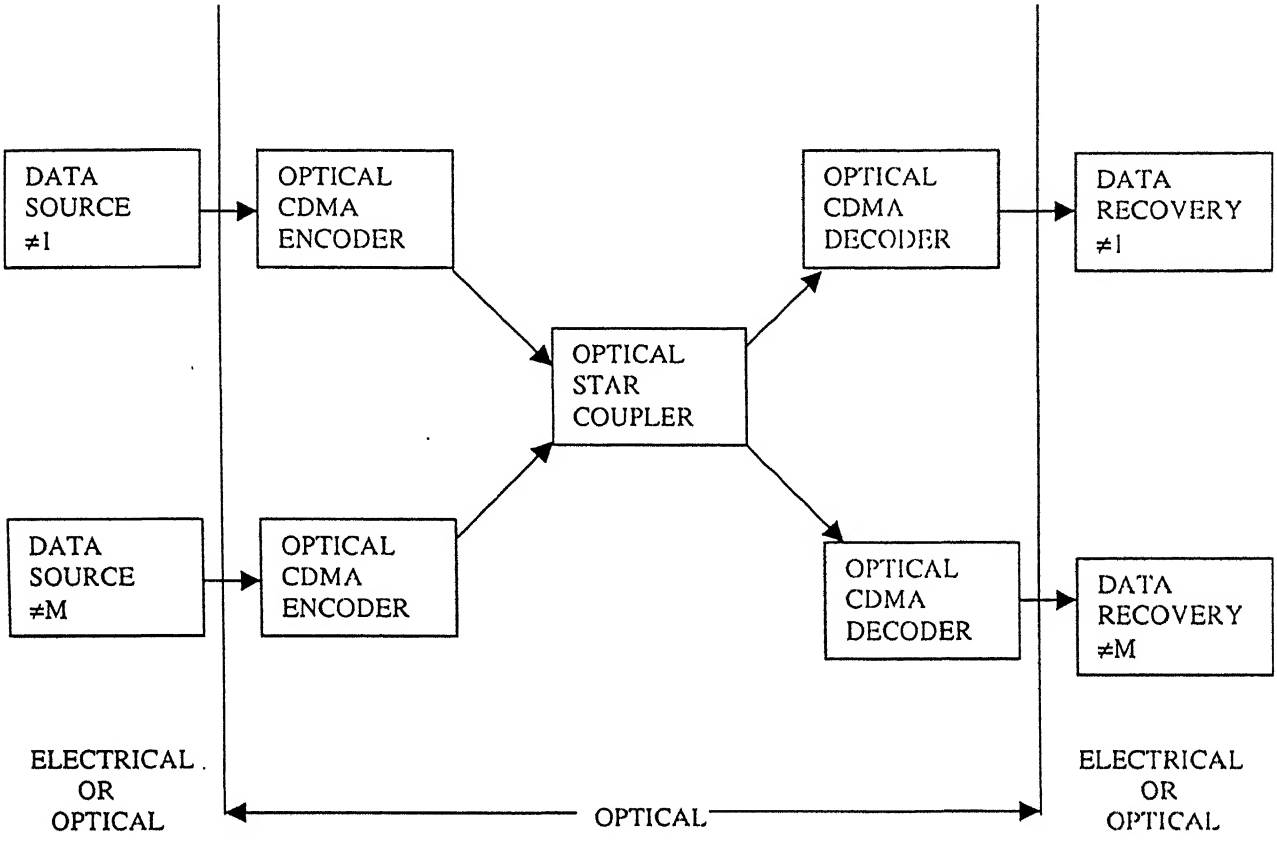

Figure 2.2.1 A FO-CDMA Network in Star configuration

2.2.1 GOLD CODE

The experimental study of Gold codes has been done in [12]. In this work Gold codes have been studied for their suitability in OCDMA. As Gold code family member codes do not have fixed number of ones, so the auto and crosscorrelation peaks are different for different members. Also the number of ones in a code nearly equal the number of zeros, therefore autocorrelation peaks are higher than OOCs which is a favourable thing. But the crosscorrelation peaks are also very high and hence Gold codes are unsuitable for OCDMA. The formula for SNR of the Gold codes is evaluated as

$$SNR_{conventional} = \frac{4F^3}{(N-1)(K^2+K-1)} \qquad (2.2.1)$$

As seen from the expression for a given code length (F), as the number of users increases SNR decreases, i.e., the performance of the system deteriorates.

2.2.2 PRIME CODE

The prime codes are called so as they are generated taking a prime number as the weight of code. The length of the code is equal to the square of a prime number. The prime codes are constructed relaxing the crosscorrelation constraint to λ_c=2,this increases the number of codes in a family, but simultaneous users are nearly half as compared to the case with λ_c=1. So they can be useful if there are a large number of users but the simultaneous users are less. OCDMA using (32,5,1,2) as parameter was studied in [12]. The peak of autocorrelation function obtained was five (as expected) and the crosscorrelation peak obtained was two (as per design) if two particular codes of this family are taken. The value of the variance of crosscorrelation amplitude was obtained as 0.29 by using all possible codes of family and different values of weight of code. The SNR for the prime codes corresponds to ratio of square of the peak of autocorrelation function to the variance of the amplitude of crosscorrelation for (N-1) uncorrelated interferers.

$$SNR_{optical} \approx \frac{1}{0.29}\frac{K^2}{(N-1)} \qquad (2.2.2)$$

So the SNR using optical processing increases in proportion to increase in chips per bit. In [12] conventional CDMA and OCDMA are also compared. It is shown that with F=31 in conventional, and for a comparable optical system with F=961(due to increase in processing speed), for BER=10^{-8}, 2 users in conventional while 26 in OCDMA can be accommodated. This establishes the advantage of OCDMA over conventional systems.

2.2.3 QUASI-PRIME CODE

These codes were studied in OCDMA system in [6]. In the experimental set-up the codes were generated with the fiber optic lattice using 3dB electro-optic couplers as encoders. The BER was calculated assuming intersymbol interference to be the dominant source of error. Interference contributions were treated as independent random variables, the statistics of which are known from the crosscorrelation functions of code. It is found that they have better performance than prime codes for lower weights because although autocorrelation peak increases with weight, crosscorrrelation functions are virtually unaffected. For higher weights, the performance of quasi-prime codes is degraded due to the non-uniformity of code pulses but this is offset by the high efficiency of the lattice as an encoder and decoder when compared to other topologies. That is, a reduction in interference rejection for a given code length is traded for improved SNR due to lower insertion loss by the encoder and decoder elements.

2.2.4 ULTRA SHORT PULSE CDMA

The optical CDMA using femtosecond pulses is described in [3]. It uses the encoder and decoder doing coding in frequency domain. The temporal shaping of coherent ultra short pulses has been previously utilized [16]. At the transmitter end a coherent ultra short pulse representing one bit of information was directed to the optical encoder, which consists of a pair of diffraction gratings, placed at the focal planes of a unit magnification confocal lens pair. The first grating spatially decomposes (with a certain resolution) the spectral components which constitute the input ultra short pulse, see Figure (2.2.2). A pseudo random spatially patterned phase mask was inserted midway between the lenses at the point where the optical spectral components experience maximum spatial separation. Thus, the mask introduces pseudo random phase shifts among the different spectral components. After the phase mask the spectral components were reassembled by the second lens and second grating into a single optical beam. The Fourier transform of the pattern transferred gives the temporal profile of the encoded pulses emerging from the grating and lens apparatus, by the mask onto the spectrum. Thus pseudo random phase mask transforms the incident pulse into a low intensity PN burst. There is a different mask for the different user.

The receiver consists of an optical decoder similar to encoder except conjugate phase mask is used here. In case the masks match (i.e. conjugate relation is there) the pulse is decoded, otherwise spectral phase shifts are rearranged but not removed and output is still a lower intensity noise PN burst. The threshold device is set to detect data corresponding to intense properly decoded pulses, and to reject low intensity improperly decoded PN bursts.

Assuming 310 Mbps individual data rate of users it has been estimated that utilizing 400 element random codes 300 subscriber pairs can be accommodated at a BER of 10^{-10} for input pulse with width 80femtosecond. Further, by increasing code length the system performance improves dramatically, hence more users can be accommodated.

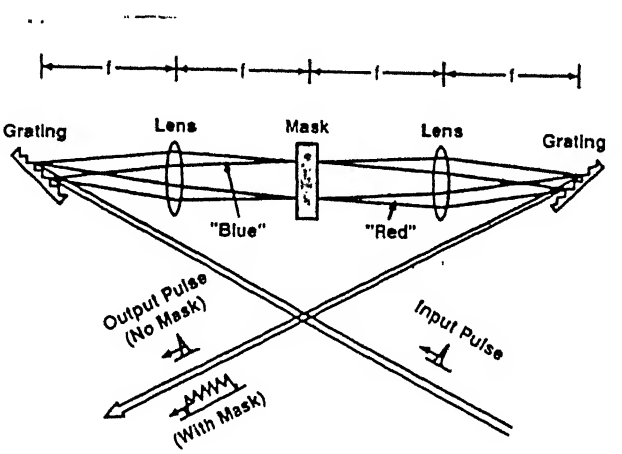

Figure 2.2.2 Ultra short pulse encoding apparatus

CHAPTER 3

TYPICAL FIBER OPTIC CDMA LINK

A typical fiber optic CDMA link is discussed in this chapter. Refer to Figure 2.2.1, which shows a typical OCDMA system. In this system a link can be represented as in Figure 3.1

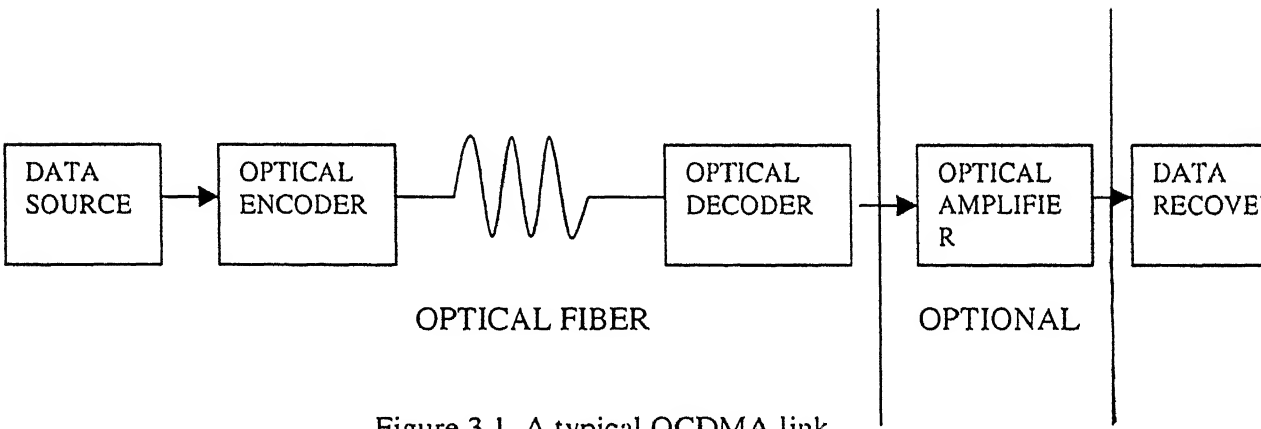

Figure 3.1 A typical OCDMA link

The important components used are

- Data source (electrical or optical)
- Optical encoder
- Fiber span
- Optical decoder (matched filter)
- Optical preamplifier (optional)
- Optical receiver for data recovery

We will discuss these elements one by one in detail.

3.1 DATA SOURCE

The source of data can be any information source and can have as low bandwidth as an audio channel to as high bandwidth as a video channel. The data is to be converted to optical signal, which can be achieved by using an optical transmitter like LED and

semiconductor laser. For our use laser diode is suitable as it can emit high power (≈10mW) in addition to coherent nature of light output. A mode locked laser produces a low duty cycle, high intensity pulse stream at the data rate. One can achieve intensity modulation by modulating the supply current to the laser diode. The wavelength of operation is λ=1550nm.

We will be using single mode fiber with attenuation coefficient 0.2 dB/Km. The fiber attenuation is taken as the dominant propagation loss.

3.2 OPTICAL ENCODER AND DECODER

The OOCs cannot be generated using shift register, as is the case with PN sequences. The encoding of the data bits is done by coupled optical delay lines. In order to understand how is encoding and decoding done, we will analyse two single mode optical fibers mutually coupled at F positions along their length as shown in Figure 3.2. L_{mn} identifies the length (delay) of each segment

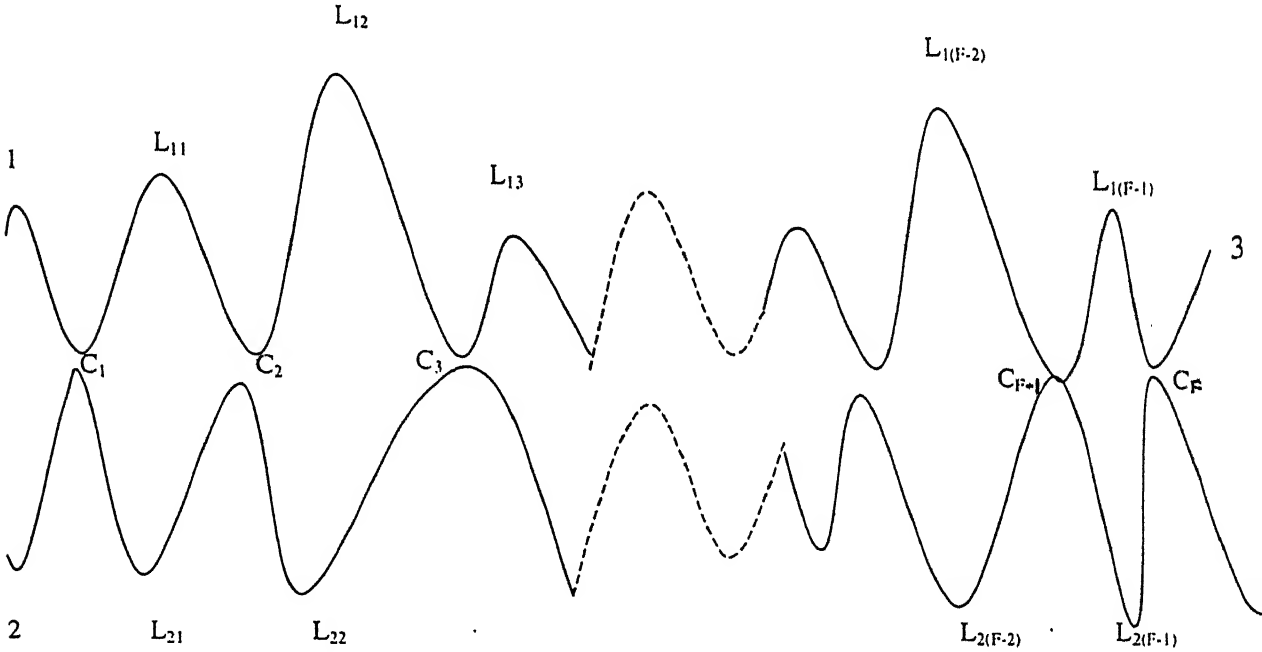

Figure 3.2.1 Optical encoder and decoder

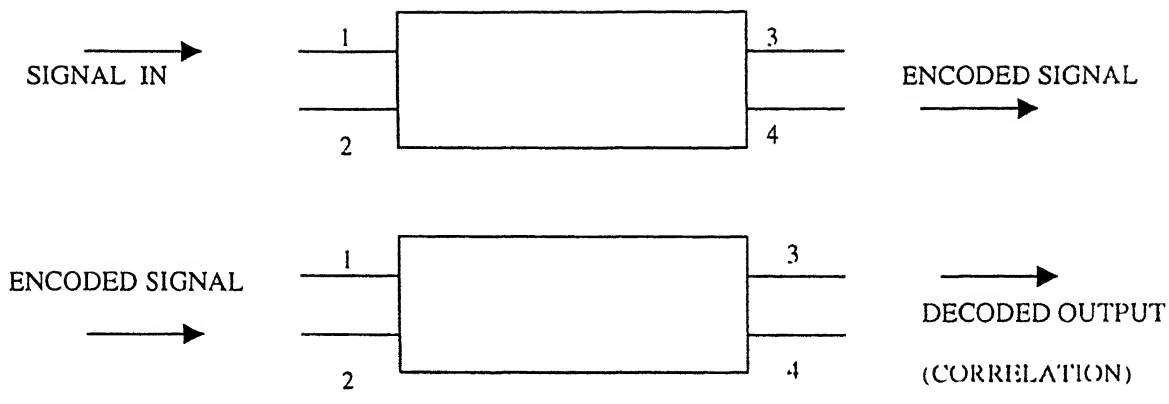

Figure 3.2.2 Schematic notation of utilization of two single mode coupled lines for encoding/decoding information.

Assuming that F couplers have been introduced, the total length of upper line is

$$L_{1T} = \sum_{n=1}^{F-1} L_{1n} \qquad (3.2.1)$$

with a corresponding time delay

$$\tau_{1T} = \frac{1}{v} \sum_{n=1}^{F-1} L_{1n} \qquad (3.2.2)$$

where v is the velocity of propagation of light in the fiber. Similarly the lower delay line has length

$$L_{2T} = \sum_{n=1}^{F-1} L_{2n} \qquad (3.2.3)$$

and a total time delay

$$\tau_{2T} = \frac{1}{v} \sum_{n=1}^{F-1} L_{2n} \qquad (3.2.4)$$

Assuming that coupling coefficient (α_n) at each coupling connection is much smaller than the transmission coefficient (β_n), we can evaluate the impulse response at terminal 3 and 4. This assumption is done as a requirement for optimal energy transfer [11]. Thus for a pulse input at the port 1 ($i_{11}(t)=\delta(t)$) we have

$$i_{31}(t) = \prod_{k=1}^{F} \beta_k \delta(t - \tau_{1T}) = A\delta(t - \tau_{1T}) \qquad (3.2.5)$$

$$i_{41}(t) = \sum_{n=1}^{F} a_n \delta(t - \tau_n) \qquad (3.2.6)$$

with $$a_n = \left[\prod_{k=1}^{n-1} \beta_k\right] \alpha_n \left[\prod_{k=n+1}^{F} \beta_k\right] = \frac{\alpha_n}{\beta_n}\left[\prod_{k=1}^{F} \beta_k\right] = \frac{\alpha_n}{\beta_n} A \qquad (3.2.7)$$

and $$\tau_n = \frac{1}{v}\left(\sum_{q=1}^{n-1} L_{1q} + \sum_{p=n}^{F-1} L_{2p}\right) \qquad (3.2.8)$$

Equation (3.2.6) describes a signal, which is coded version of input pulse at port1. We can choose $a_n \in \{0,1\}$ such that at output port 4 we get encoded data. Thus by selecting K taps from any of the F positions one can get an encoder for a particular user's code.

Now we will establish that if coded data is fed at port 2 of the same arrangement, decoded output can be retrieved at port 3.

Taking transform of equation (3.2.6)

$$I_{41}(\varpi) = \sum_{n=1}^{F} a_n e^{-i\varpi\tau_n} \qquad (3.2.9)$$

Thus the transfer function of decoding matched filter should be

$$I_{41}^{*}(\varpi) = \sum_{n=1}^{F} a_n e^{+i\varpi\tau_n} \qquad (3.2.10)$$

So the desired filter in time domain is

$$f(t) = \sum_{n=1}^{F} \int a_n e^{i\varpi\tau_n} e^{-i\varpi\tau_n} d\varpi$$

$$= \sum_{n=1}^{F} a_n \delta(t + \tau_n) \qquad (3.2.11)$$

For evaluating the transfer function from terminal 2 to terminal 3, we feed a pulse at terminal 2 . Now we get

$$i_{32}(t) = \sum_{m=1}^{F} d_m \delta(t - \bar{\tau}_m) \qquad (3.2.12)$$

where $$d_m = \left\{\prod_{k=1}^{m-1}\beta_k\right\}\alpha_m\left\{\prod_{k=m+1}^{F-1}\beta_k\right\} = \frac{\alpha_m}{\beta_m}\left\{\prod_{k=1}^{F}\beta_k\right\} \equiv a_m \quad (3.2.13)$$

and $$\bar{\tau}_m = \frac{1}{v}\left\{\sum_{p=1}^{m-1}L_{2p} + \sum_{q=m}^{F-1}L_{1q}\right\} \quad (3.2.14)$$

It is clear that $\bar{\tau}_m$ is a complementary function to τ_m since the order of delay is reversed: the first (m-1) delays originate from the lower line and the last (N-m) ones are from the upper one. Thus by simple mathematical manipulation [12] we get

$$\bar{\tau}_m = T - \tau_m \quad (3.2.15)$$

where T is the sum of total delays of two lines.
Substituting (3.2.13) and (3.2.15) in(3.2.12) we get

$$i_{32}(t) = \sum_{m=1}^{F} a_m \delta(t - T + \tau_m) \quad (3.2.16)$$

which is of identical form to that required by (3.2.11) except for a constant time delay T.

Thus the output signal detected at port 3 after transmitting a signal from port 1 to 4 and then again from port 2 to 3 is expressed by

$$\begin{aligned} i_{31}(t) &= \sum_{n=1}^{F}\sum_{m=1}^{F} a_n a_m \delta(t-\tau_n) \otimes \delta(t - T + \tau_m) \\ &= \sum_{n=1}^{F} a_n{}^2 \delta(t-T) + \sum_{n=1, n\neq m}^{F}\sum_{m=1}^{F} a_n a_m \delta(t - T + \tau_m - \tau_n) \end{aligned} \quad (3.2.17)$$

The F terms corresponding to n=m occuring simultaneously at t=T form the autocorrelation part. The other (F^2-F) terms distributed over the interval 2T provide the crosscorrelation background. The choice of the delay line lengths $\{L_n\}$ establishes the distribution of the crosscorrelation terms.

3.3 OPTICAL AMPLIFIER

Optical amplifiers provided a key to optical communication overcoming the bandwidth limitations of electronic repeaters whose main functions are retiming, reshaping, and regeneration.

The various types of optical amplifiers are

- SLA (Semiconductor Laser Amplifier)

- EDFA (Erbium Doped Fiber Amplifier)
- Raman and Brillouin Amplifiers

Among these, EDFA has several advantages over others viz.

1. EDFA have a large GBW (gain bandwidth) product. They can provide high gains over a bandwidth of 40nm.
2. Fiber amplifiers can be easily spliced to the telecommunication fiber link with minimal insertion losses.
3. The noise added by the amplifier is close to the lowest possible value (3-4 dB).
4. The fiber amplification process is controlled by discrete atomic lines rather than by continuous energy bands, as with SLA, therefore the former has gain with smaller sensitivity to temperature.
5. The gain provided by EDFA is independent of polarization of input signal.

The following are drawbacks of EDFA

1. Currently they are limited to 1550nm operating wavelength only. For systems with 1330nm operating wavelength, efforts are underway to develop amplifiers based on other rare earth elements as dopant like praseodymium.
2. They require high pump powers (50-100mW).
3. Very short physical length of EDFA is not possible; approximately 30-40m long fiber is used in practice.

3.3.1 GAIN SPECTRUM AND GAIN BANDWIDTH

The gain of an EDFA depends on pump power, input power, and emission and absorption cross-section of the fiber of amplifier. As these cross-sections are function of wavelength, so the gain is also dependent on wavelength of the signal. The spectral response of EDFA for various values of pump power is shown in Figure 3.3.1.

The curve shows that for a given input pump power, the fiber exhibits gain for wavelengths greater than a specific wavelength and exhibits attenuation for wavelengths shorter than this cut-off wavelength. As the pump power increases the specific wavelength for which net gain is zero (neither amplification nor attenuation) moves towards shorter wavelength.

3.3.2 CONFIGURATION OF OPTICAL AMPLIFIERS

The EDFA can be used in following three modes

1. Power amplifier to boost the source power at the transmitter end just after the source. In this configuration high output power is achieved at the expense of reduced gain (gain

saturation due to high source power) and increased noise figure. For better performance backward pumping or even bi-directional pumping can be used.

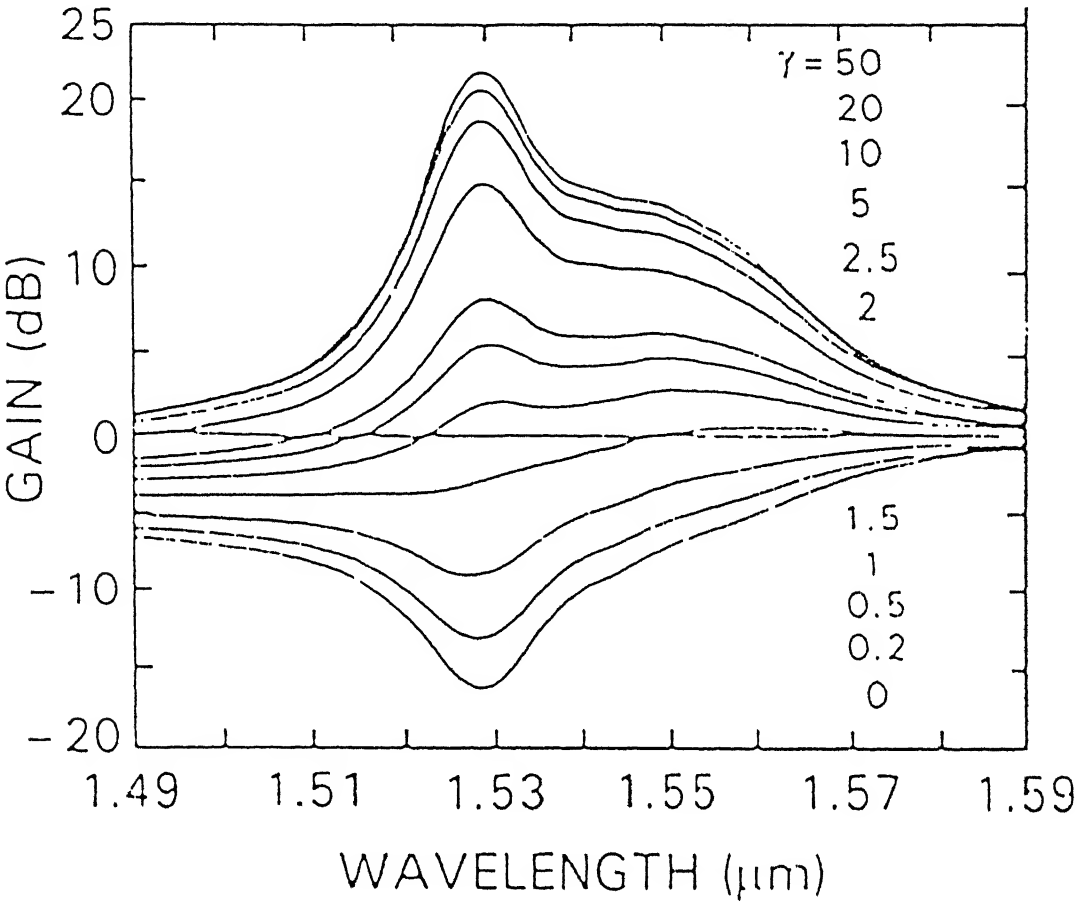

Figure 3.3.1 Spectral response of an EDFA [17]

2. Preamplifier to improve the receiver sensitivity used just before the receiver. It is operated in unsaturated regime. The requirement for this use is good noise figure.
3. In line amplifier, to amplify signals enroute i.e. as a repeater. Optical band pass filters are used in this configuration to reduce the accumulation of amplified spontaneous noise (ASE).

We will be using EDFA as a preamplifier. The use of optical amplifier as preamplifier instead of avalanche photodiode (APD) is guided by the fact that APD are limited by their gain-bandwidth product. The EDFA in our use has to be operated at 1550nm. The gain model of EDFA is given in Appendix A.

3.3.3 NOISE CONSIDERATIONS IN OPTICAL AMPLIFIERS

With electronic amplifiers the noise is a consequence of the random nature of thermal motion of electrons in the input resistor, or of the random process inside the amplifier itself, analogous to the thermionic shot noise in a vacuum tube. For the photonic amplifiers the dominant noise is amplified spontaneous emission (ASE). Spontaneous noise is generated in all the portions of gain medium, but the part of the spontaneous noise that most degrades the system performance is that generated at points near the amplifier input, where the signal is still weak.

The spontaneous noise in amplifier can be modeled as a stream of random arrivals, each an infinitely short impulse, so that the power spectrum of noise at the point of generation within the amplifier is flat with frequency. It has been shown (See Appendix A) that the amplifier noise output power spectral density is

$$S_{sp}(f)df = hfn_{sp}(G(f)-1)df \text{ Watts} \qquad (3.3.18)$$

where,
G (f) is the gain at frequency f
n_{sp} is spontaneous emission factor also called population inversion factor (signifying less complete the population inversion more the spontaneous noise).

An optical filter is placed after photonic amplifier to reduce the ASE noise adding to the amplified signal. We have chosen its bandwidth to be 1THz.

3.4 OPTICAL RECEIVER

The optical receiver consists of a detector, which can be a PN diode, a PIN diode or an Avalanche photo detector, followed by a decision circuit (also called threshold device) which retrieves back the bit transmitted. The detection principle of all detectors is same as photodiode, in which, ideally, for every photon (with energy>bandgap) incident on reverse biased junction, an electron-hole pair is generated. The electrons flow out of the photodiode and into the external circuit and produce a useful photo detected signal. In order to enlarge the depletion region a layer of intrinsic material is sandwiched between n and p region giving birth to PIN diode.

A detector is characterized by its reponsivity, which is the degree to which it approaches the ideal of one electron generation per incident photon. Mathematically

$$R = \frac{I}{P} = \frac{\eta q}{h\nu} \qquad (3.4.1)$$

η is called quantum efficiency of detector. Its practical value is 0.60-0.80. It is a function of wavelength and device parameters such as reflectivity of the facet through which the light must pass before entering the device, depth of p region, depth of depletion region, and material of detector.

3.4.1 NOISE IN DETECTION PROCESS

The conversion process from light to electrical current is accompanied by the addition of noise. The two most important noise mechanisms in a photo detector circuit are shot noise and thermal noise.

1. SHOT NOISE

This noise is accounted to the fact that electric current is nothing but a stream of discrete charges (electrons) which are randomly generated. Thus the detection statistics modifies the random photon arrival statistics (quantum noise)- which is Poisson distributed- resulting in a new statistics. The mean of this statistics is
$\langle i_{sh}(t) \rangle = e\langle n \rangle$, where $\langle n \rangle$ is time averaged electron count rate over infinite interval.

The variance is

$$\langle i^2_{sh} \rangle = 2e(I + I_d)\Delta f \qquad (3.4.2)$$

where

I is average current generated in photo detector.
I_d is dark current in photo detector, which is current in photo detector without any light radiation incident on it. It arises from thermally generated carriers and increase with temperature. Typical value is tens of nA.
Δf is bandwidth over which noise is considered.
e is electron charge.

2. THERMAL NOISE

It arises in the load resistor of the photodiode circuit due to random thermal motion of electrons. Since motion of electrons constitutes current, so random thermal motion leads to random current in resistor. This current has zero mean and its mean square noise is given by

$$\langle i^2_{th} \rangle = \frac{4K_B T \Delta f}{R_L} \qquad (3.4.3)$$

where

K_B is Boltzman constant.
R_L is load resistance.
Δf is bandwidth over which noise is considered.
Note that thermal noise is independent of incident optical power.

In addition to these due to square law detection by the receiver, the ASE noise of the amplifier produces beat noises which have the values given by

Beat term of ASE with itself

$$\sigma^2_{sp-sp} = 4R^2 S_{sp}{}^2 \Delta\upsilon_{opt} \Delta f \qquad (3.4.4)$$

Beat term of ASE with signal

$$\sigma^2_{sig-sp} = 4R^2 G P_s S_{sp} \Delta f \qquad (3.4.5)$$

Beat term of ASE with shot noise

$$\sigma^2_{sh-sp} = 4qRS_{sp} \Delta\upsilon_{opt} \Delta f \qquad (3.4.6)$$

here

$\Delta\upsilon_{opt}$ is the bandwidth of ASE noise
Δf is electrical bandwidth of detector
S_{sp} is ASE noise power spectral density
R is responsivity of detector
G is gain of optical amplifier
P_s is signal power

In the next chapter we will analyze the OCDMA link using the characteristics of the various elements described in this chapter.

CHAPTER 4

PERFORMANCE ANALYSIS OF OCDMA LINK

In this chapter we will analyze mathematically the OCDMA link as shown in Figure 2.2.1.In a typical Fiber Optic CDMA (FO-CDMA) system, there would be N transmitter and receiver pairs (users). The network topology can be star configuration.

4.1 ASSUMPTIONS

For the performance analysis i.e. the bit error rate calculations, we consider the simplest network protocol: it is assumed that the communication between each n_{th}, for $1 \leq n \leq N$, transmitter and receiver is continuous. The optical intensity of multiple users occurring at same time would add up coherently. Furthermore, all users have the same effective average power at the input of any receiver so that one user's signal cannot overwhelm the signal from other users.

4.2 TRANSMITTER END

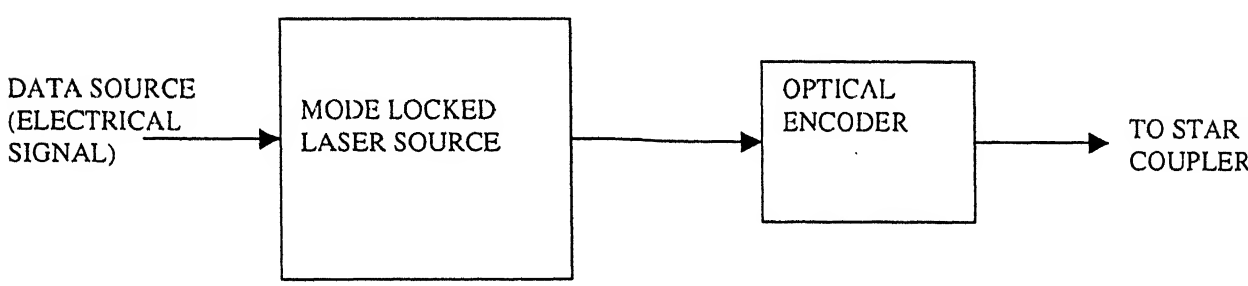

Figure 4.2.1 Block schematic of the Transmitter

A particular user's data intensity modulates a laser diode output (See Figure 4.2.1) to give a stream of optical pulses. These pulses are encoded by his signature sequence using tapped delay line encoder, described in Section 3.2. Similarly we have other transmitter units for other users with their own signature for encoding. These signals are combined by a star-coupler (See Figure 4.2.1).

The n^{th} baseband signal, $s_n(t)$, at the output of the n^{th} optical encoder is given by

$$s_n(t) = s_n b_n(t) DP_n(t) \qquad (4.2.1)$$

where

s_n is n^{th} user's transmitted optical intensity

$b_n(t)$ is binary data signal of n^{th} user

$DP_n(t)$ is OOC for n^{th} user

For continuous communication, data signal $b_n(t)$ is given by

$$b_n(t) = \sum_{l=-\infty}^{\infty} b_l^{(n)} P_T(t - lT) \qquad (4.2.2)$$

Here $(b_l^{(n)})$ is the n^{th} data sequence that takes the value 0 or 1(On-off keying) for each l with equal probability, and $P_T(t)$ denotes a pulse of width T starting at t=0

Further $DP_n(t)$, the n^{th} users OOC (signature sequence) is given by

$$DP_n(t) = \sum_{j=-\infty}^{\infty} A_j^{(n)} P_{T_c}(t - jT_c) \qquad (4.2.3)$$

where

$P_{T_c}(t)$ is a pulse of duration T_c and

$(A_j^{(n)})$ is the n^{th} periodic sequence of binary optical pulses (0,1) with period (length) $F = \frac{T}{T_c}$, i.e.

$$A_{j+F}^{(n)} = A_j^{(n)} \text{ and weight K}$$

4.3 RECEIVER END

Figure 4.3.1 shows the block diagram of a particular user say user 1's receiver. The signal received is correlated to his signature sequence. This is equivalent to a matched filter whose impulse response is reflection of the signature sequence about t=0 and delayed by t=T. The output of correlator is amplified by photonic amplifier, followed by a photo

detector (PIN diode in our case), and then sampled at t=T. The threshold detector takes a decision whether the received bit is 0 or 1.

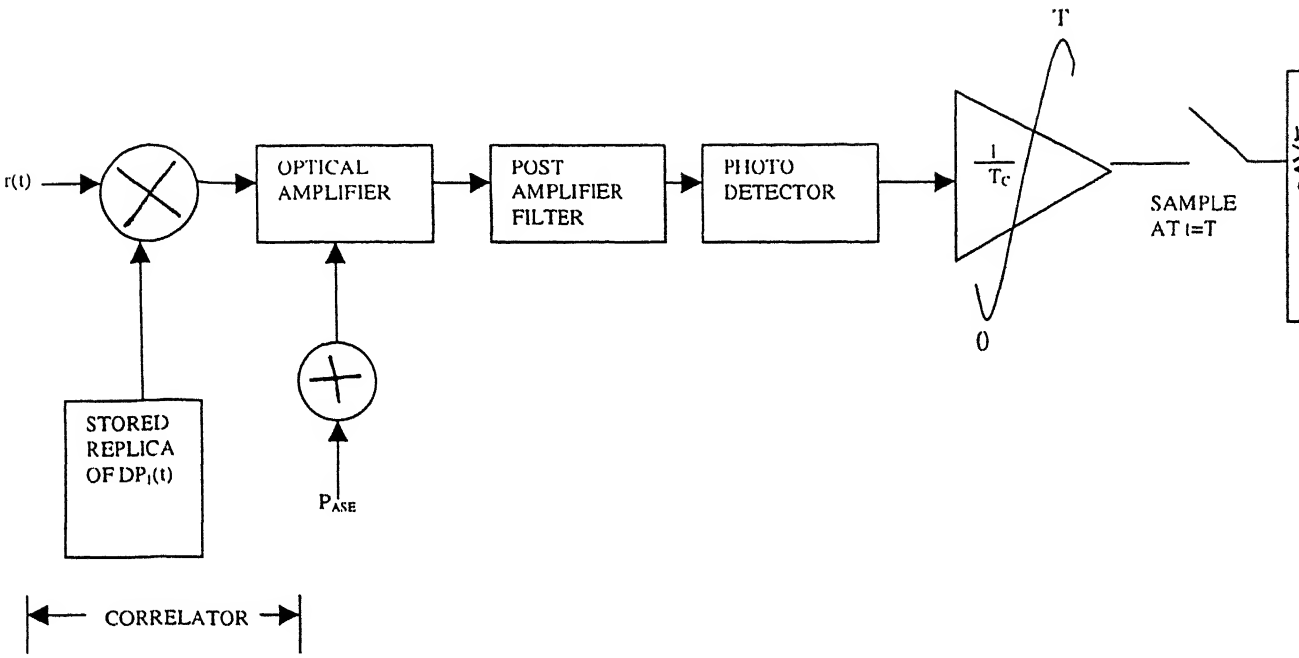

Figure 4.3.1 Receiver of user 1 in OCDMA

As the transmitters are not time synchronous (with each other), so the received signal at the front end of each receiver is of the form

$$r(t) = \sum_{n=1}^{N} s_n(t-\tau_n) \qquad (4.3.1)$$

where τ_n is the delay associated with the n^{th} user
From Eqn.(4.2.1) and (4.3.1) we have

$$r(t) = \sum_{n=1}^{N} W_n b_n(t-\tau_n) DP_n(t-\tau_n) \qquad (4.3.2)$$

Here, W_n is the optical intensity received after various losses such as fiber attenuation, coupling losses, connector losses, pigtail losses, etc.

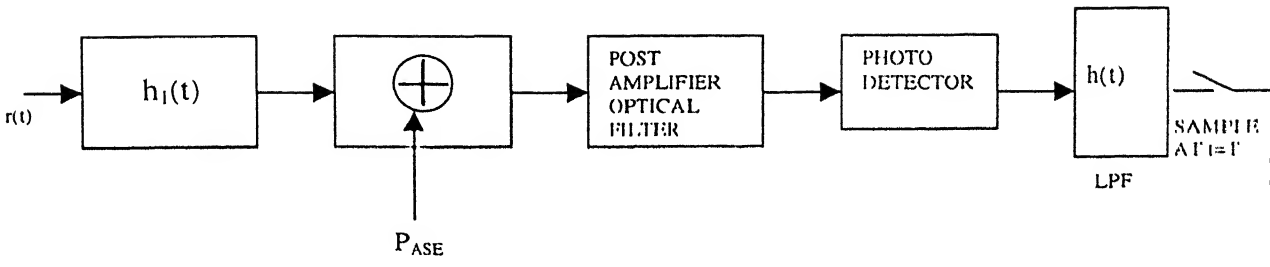

Figure 4.3.2 Equivalent matched filter version of receiver of user 1, $h_1(t)$ is impulse response of matched filter which is equal to the delayed version of user 1's signature

4.3.1 OPTICAL CORRELATOR

The effect of n^{th} user's signal on the first user receiver is denoted by $I^{(1)}{}_n$. Hence the output of the first user's correlator at time T, can be written as

$$Z_1 = \frac{1}{T_c}\int_0^T r(t)DP_1(t)dt$$

$$= W_n b_0^{(1)} K + I_1 \qquad (4.3.3)$$

where $b_0^{(1)}$ is the zeroth data bit of the fist user, which can take on two values, 0 or 1 with equal probability. The first term of (4.3.3), $b_0^{(1)}K$, is the desired signal term and the second term $I_1 = \sum_{n=1}^{N} I_n^{(1)}$ is the undesired signal term (total interference signal) at the output of the desired receiver's correlator i.e. user 1's receiver. The interference signal is a random variable whose distribution is derived in Appendix B.

In OCDMA system, the correlation output of the signal of the other users with the code of desired user is the interference signal for the desired user. The output of the equivalent matched filter is a random variable. The exact evaluation of probability density function for I_1, the interference signal for the user 1, will require the knowledge of pdf associated with each $I_n^{(1)}$, for $2 \leq n \leq N$, since there are N users in the FO-CDMA system. The interference I_j at the output of the j^{th} receiver contains (N-1) interference terms so a total knowledge of N(N-1)/2 pdfs would be required. This task is lengthy and tedious for large N. Therefore two extreme cases for the analysis of interfering signals are chosen to make the calculations on probability density and associated BER mathematically more

convenient. These cases are chip synchronous and chip asynchronous interferences. The mean and variance of intensity of interference signals (See Appendix B) is reproduced below.

If the net interference on user 1 is denoted by $I = \sum_{n-2}^{N} I_n$ then,

$$E\{I_1\} = E\left\{\sum_{n=2}^{N} I_n^{(1)}\right\} = \begin{cases} (N-1)\dfrac{K^2}{2F} W_n \, for, chip - sym. \\ (N-1)\dfrac{K^2}{F} W_n \, for, chip - asyn. \end{cases} \quad \text{(B.15)}$$

$$\text{var}(I_1) = \text{var}\left(\sum_{n=2}^{N} I_n^{(1)}\right) = \begin{cases} W_n^{\,2}(N-1)\dfrac{K^2}{2F}\left(1 - \dfrac{K^2}{2F}\right) for, chip - sym. \\ W_n^{\,2}(N-1)\dfrac{2K^2}{F}\left(\dfrac{1}{3} - \dfrac{K^2}{2F}\right) for, chip - asyn. \end{cases} \quad \text{(B.16)}$$

4.3.2 OPTICAL AMPLIFIER AND OPTICAL FILTER

The optical amplifier we have incorporated in the system is an EDFA, which is a broad band amplifier, as described in the previous chapter (See Figure 3.3.1). It has 25nm bandwidth around 1550nm wavelength and hence for our analysis we can assume it to be flat gain amplifier, under restriction that gain saturation effects do not get manifested. After amplification both desired and interfering signals get amplified.

So the desired signal optical intensity after amplification is, see eqn. (4.3.3)

$$Z_1' = GW_n b_0^{(1)} K \quad \text{(4.3.4)}$$

The interfering signal will be amplified such that both mean and variance will change. The output signal intensity has mean and variance given by

for chip synchronous case

$$m_a = GW_n \frac{K^2}{2F}(N-1) \quad \text{(4.3.5)}$$

$$\sigma^2{}_a = G^2 W_n^{\,2} \frac{K^2}{2F}\left(1 - \frac{K^2}{2F}\right)(N-1) \quad \text{(4.3.6)}$$

and for chip asynchronous case

$$m_a = GW_n \frac{K^2}{F}(N-1) \tag{4.3.7}$$

$$\sigma^2{}_a = G^2 W_n{}^2 \frac{2K^2}{F}\left(\frac{1}{3} - \frac{K^2}{2F}\right)(N-1) \tag{4.3.8}$$

Further the amplifier will introduce ASE noise whose psd is given by

$$S_{sp} = (G-1)n_{sp}h\upsilon \tag{3.2.18}$$

So the optical noise power added after filtering is

$$P_{sp} = (G-1)n_{sp}h\upsilon\Delta\upsilon_{sp} \tag{4.3.9}$$

4.3.3 PHOTODETECTOR

The count statistics of a photo detector is Poisson distributed. The probability of K photoelectrons being generated is given by [14]

$$P_K(k) = \frac{(m_v)^k}{k!}e^{-m_v} \qquad k \geq 0 \tag{4.3.10}$$

where

$$m_v = \alpha \int_V I(\mathbf{v})d\mathbf{v} \tag{4.3.11}$$

where, $I(\mathbf{v})$ is optical intensity at a point in three-dimensional space, with two dimensions corresponding to area of photo detector and third dimension for the observation time. m_v is called level of probability.

α is a constant $= \dfrac{\eta}{h\upsilon}$

η is quantum efficiency of photo detector

h is Planck's constant

υ is frequency of operation

If the value of optical intensity at any arbitrary point in above space is given by $I(t,\mathbf{r})$, then we normalize it such that the normalized intensity will be directly related to m_v, i.e.,

$$n(t,\mathbf{r}) = \alpha I(t,\mathbf{r}) \tag{4.3.12}$$

$$\therefore m_v = \int_A \int_t^{t+T} n(\rho,\mathbf{r})d\rho d\mathbf{r} \tag{4.3.13}$$

We can also define the spatially integrated count intensity as

$$n(t) = \int_A n(t,\mathbf{r})d\mathbf{r} = \alpha \int_A I(t,\mathbf{r})d\mathbf{r} \qquad (4.3.14)$$

So m_v can be expressed in compact form as

$$m_v = \int_t^{t+T} n(\rho)d\rho \qquad (4.3.15)$$

If the optical intensity is not constant but has temporal variations, then we can invoke short term conditional Poisson counting (conditional Poisson, because of assumption in Section 4.3.10 that count statistics is conditioned on a known value of m_v, which is true only if intensity is constant with respect to time, but, if intensity is a stochastic process then this is not true). This is done for simplifying calculations under assumption of point detector and "short term" counting instants.

Let us denote point detector area as A and counting interval as T. We define a short term counting time as a value of time T for which the integral of intensity process n(t) over (t,t+T) is approximately equal to n(t)T, i.e., we have short term counting condition if T is such that

$$m_v = \int_t^{t+T} n(\rho)d\rho \approx n(t)T = \alpha IAT \qquad (4.3.16)$$

Here I is intensity of incident light.

If incident power (a random variable, Gaussianly distributed with mean P_0 and variance σ^2) is P then

$$m_v = \alpha PT \qquad (4.3.17)$$

For mathematical convenience of analysis, let

$$U = \alpha P \qquad (4.3.18)$$

So the probability distribution of random variable U is related to probability distribution of incident power by

$$p_U(u) = \left.\frac{p_P(P)}{\alpha}\right|_{P=\frac{u}{\alpha}} \qquad (4.3.19)$$

$$p_P(P) = \frac{1}{\sigma\sqrt{2\pi}} e^{\frac{(P-P_0)^2}{2\sigma^2}} \qquad (4.3.20)$$

$$\therefore p_U(u) = \frac{1}{\alpha\sigma\sqrt{2\pi}} e^{-\frac{\left(\frac{u}{\alpha}-P_0\right)^2}{2\sigma^2}} \qquad (4.3.21)$$

Finding the expectation of u

$$E\{U\} = \frac{1}{\alpha\sigma\sqrt{2\pi}} \int_0^\infty u e^{-\frac{\left(\frac{u}{\alpha}-P_0\right)^2}{2\sigma^2}} du$$

The integral can be evaluated as a sum of two integrals which are

$$I_1 = \alpha^2 \int_{-P_0}^{\infty} v e^{-\frac{v^2}{2\sigma^2}} dv$$

$$I_2 = P_0\alpha^2 \int_{-P_0}^{\infty} e^{-\frac{v^2}{2\sigma^2}} dv$$

where $v = \frac{u}{\alpha} - P_0$

On solving these integrals we get

$$E\{U\} = \frac{\alpha\sigma}{\sqrt{2\pi}} e^{-\frac{P_0^2}{2\sigma^2}} + P_0 \frac{\alpha}{2} erfc\left(\frac{P_0}{\sqrt{2\sigma^2}}\right) \qquad (4.3.22)$$

Now the expectation of the number of counts E{k} is given as [14]

$$E\{K\} = E\{m_v\}$$

$$\therefore E\left\{\frac{K}{T}\right\} = E\left\{\frac{m_v}{T}\right\} = E\{U\}$$

The average particle count/time when multiplied by the charge of particle (electron) will give the mean current registered in the detector, i.e.,

$$E\{I\} = \bar{I} = \frac{R\sigma}{\sqrt{2\pi}} e^{-\frac{P_0^2}{2\sigma^2}} + \frac{R}{2} P_0 erfc\left(\frac{P_0}{\sqrt{2\sigma^2}}\right) \qquad (4.3.23)$$

where I is the output current of the photo detector

here $$R = \alpha\eta = \frac{\alpha q}{h\upsilon}$$

which is called the responsivity of the detector.

Similarly we can calculate the variance of the random variable U which reduces to

$$\text{var}(U) = \alpha^2\sigma^2 + P_0^2\frac{\alpha^2}{2}erfc\left(\frac{P_0}{\sqrt{2\sigma^2}}\right) + 2P_0^2\frac{\alpha^2}{\sqrt{2\pi}}e^{-\frac{P_0^2}{2\sigma^2}} - \frac{\alpha^2}{\sigma\sqrt{2\pi}}I_{numer} \qquad (4.3.24)$$

where $$I_{numer} = \int_0^{P_0} v^2 e^{-\frac{v^2}{2\sigma^2}}dv \qquad (4.3.25)$$

Now the number of particles counted/time is given by

$$\text{var}(K) = \text{var}(m_v)$$
$$\therefore \text{var}\left(\frac{K}{T}\right) = \text{var}\left(\frac{m_v}{T}\right) = \text{var}(U)$$

Therefore variance of current registered in photo detector due to optical intensity of interference signals is

$$\text{var}(I) = R^2\sigma^2 + P_0^2\frac{R^2}{2}erfc\left(\frac{P_0}{\sqrt{2\sigma^2}}\right) + 2P_0^2\frac{R^2}{\sqrt{2\pi}}e^{-\frac{P_0^2}{2\sigma^2}} - \frac{R^2}{\sigma\sqrt{2\pi}}I_{numer} \qquad (4.3.26)$$

Assuming uncorrelated nature of various noise given in Section 3.3.1 their variances will be added up to the interferers' noise variance. So the net variance of noise current is

$$\sigma_I^2 = \text{var}(I) + \sigma_{sh}^2 + \sigma_{th}^2 + \sigma_{sp-sp}^2 + \sigma_{sig-sp}^2 + \sigma_{sh-sp}^2 \qquad (4.3.27)$$

4.3.4 BER CALCULATIONS

The current at the receiver output is a fluctuating signal, which is sampled at t=T and fed to the decision circuit. The sampled value of current fluctuates from bit to bit around an average I_1 or I_0, depending on whether bit 1 or 0 was received. The decision circuit compares the sampled value with the threshold value I_d and decides 1 if $I(T) > I_d$, or 0 if $I(T) < I_d$. An error occurs if $I(T) > I_d$ for bit 0 transmitted, or $I(T) < I_d$ for bit 1 transmitted. The error occurs because of the various noises. If $\Pr(0) = \Pr(1) = \frac{1}{2}$, then bit error rate is given by

$$BER = \frac{1}{2}erfc\left(\frac{Q}{\sqrt{2}}\right) \qquad (4.3.28)$$

where $$Q = \frac{I_1 - I_0}{\sigma_1 + \sigma_0}$$

I_1 is mean current registered at the receiver for bit 1

I_0 is mean current registered at the receiver for bit 0

σ_1 is variance of current registered around mean I_1

σ_0 is variance of current registered around mean I_0

This value of BER is true for optimal setting of threshold level I_d, which is set at

$$I_d = \frac{\sigma_0 I_1 + \sigma_1 I_0}{\sigma_0 + \sigma_1} \qquad (4.3.29)$$

From Eqn.(4.3.7) and (4.3.8) we get the value of mean and variance of the intensity of interference signal, so the corresponding parameters for interference power for chip asynchronous case are

$$m_a' = AGW_n \frac{K^2}{F}(N-1) \qquad (4.3.30)$$

$$\sigma^2{}_a' = A^2G^2W_n{}^2 \frac{2K^2}{F}\left(\frac{1}{3} - \frac{K^2}{2F}\right)(N-1) \qquad (4.3.31)$$

Here A is the effective area of photo detector assuming it as a point source.

We will be analyzing further for chip asynchronous case only because in proposed system for OCDMA synchronization is not done, and the BER we will arrive at will be a lower bound. Putting the value from Eqn.(4.3.30) and (4.3.31) into Eqn.(4.3.23) and (4.3.26) respectively, we get the interference current mean $[E\{I\} = \bar{I}_{int\,rf}]$ and variance $[\mathrm{var}(I)]$ values for chip asynchronous case.

So the mean current registered by detector when bit 1 is received is, assuming that all users have equal optical intensity at the input of receiver of user 1 (W_n=W *for all n*)

$$I_1 = RKWAG + \bar{I}_{int\,rf} \qquad (4.3.32)$$

$$I_0 = \bar{I}_{int\,rf} \qquad (4.3.33)$$

From Eqn.(4.3.27) we have

$$\sigma_1 = 2q\Delta f\left(RGWAK + \bar{I}_{int\,rf}\right) + 4R^2GWAS_{sp}\Delta f\left(K + \frac{K^2}{F}(N-1)\right) + 4R^2S^2{}_{sp}\Delta\upsilon_{opt}\Delta f + \frac{4K_BT\Delta f}{R_L} + \mathrm{var}(I) \qquad (4.3.34)$$

$$\sigma_0 = 2q\Delta f\left(\bar{I}_{\text{int},j}\right) + 4R^2GWAS_{sp}\Delta f\left(\frac{K^2}{F}(N-1)\right) + 4R^2S_{sp}{}^2\Delta\upsilon_{opt}\Delta f + \frac{4K_BT\Delta f}{R_L} + \text{var}(I) \quad (4.3.35)$$

Putting these values in (4.3.28), BER can be calculated for the chip asynchronous case.

In the next chapter we will use the expression obtained for BER to study the effect of variation in various parameters on the performance of the OCDMA system.

CHAPTER 5

RESULTS AND DISCUSSION

We have plotted the bit error rate expression in the Eqn.(4.3.28) taking the number of users, weight of the code, and input power at the receiver as the parameters. The user data rate is assumed to be 155Mbps. The following list gives the various values we have used for plotting the curves using MATLAB® package.

Responsivity of detector $R = \frac{\eta q}{h\upsilon}$ =1.136 ampere/watt
Efficiency of detector $=\eta$ =0.80
Charge of electron=q=1.6 E-19 coulombs
Planck's constant $=h$ =6.62 E-34 Joule-sec
Frequency of operation $=\upsilon$ =1.935E14 Hz
Population inversion factor $=n_{sp}$ =1.4
Electrical bandwidth of detector =2.5GHz
Optical bandwidth of post amplifier filter =1THz
Boltzman constant =1.38 E –23 Joule/mole/K
Absolute temperature =300K
$S_{sp} = (G-1)n_{sp}h\upsilon$ =1.78 E –16 Watt/Hz

In choosing values of the variables, we have taken the following constraints into account:

- The number of users in the system (N) are limited by the number of OOCs that can be constructed which in turn is constrained by Eqn. (2.1.5) for a given length of code (F). For example N≤11 for F=1024 and N≤45 for F=4196.
- The power at the receiver end is lower bounded by the receiver sensitivity, -32 dBm at the PIN diode input being a typical value we have used for our purpose.
- The non-linear effects manifest themselves if the power in the fiber exceeds 1mW. So we have taken the values of power at the receiver end such that even at the transmitter end the sum of all user's power does not exceed this limit, assuming the fiber span to be greater than 10 Kms.

Now we will discuss the results we have got in the following sections.

5.1 BER VS. NUMBER OF USERS

The variation of the bit error rate with the number of users in the OCDMA system has been considered taking the input power as parameter and a code length F=10. We have plotted it for two values of the length of OOC viz. 1024 and 4096. For F=1024, as shown in Figure 5.1.1, the number of users is varied from 3 to 11. We get a nearly exponentially rising curve. If we take desired value of BER as 10^{-10} then 8 users can be accommodated in the system. The curves for the different power values coincide, which shows that the performance is independent of input power for high power values. Figure 5.1.2 shows the same plot for low power values, in which a transition in performance is observed, As power increases the performance improves, till –60dBm power input, after which the curves coincide and performance becomes independent of input power.

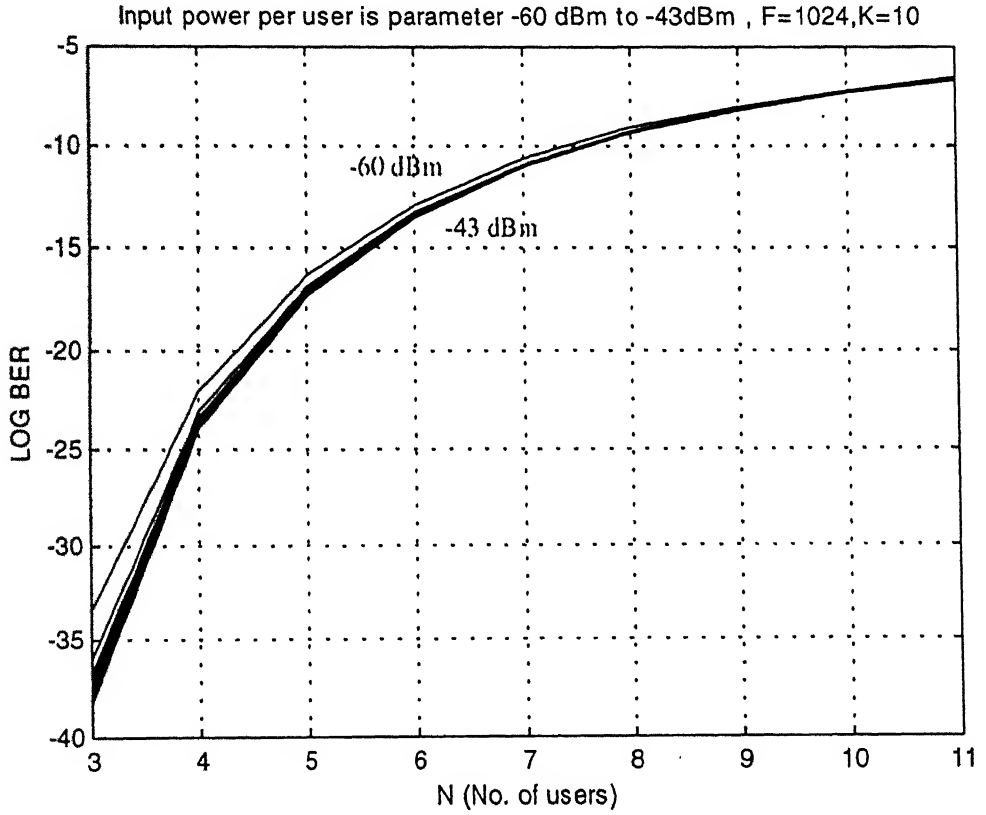

Figure 5.1.1 BER vs. Number of users for high input power

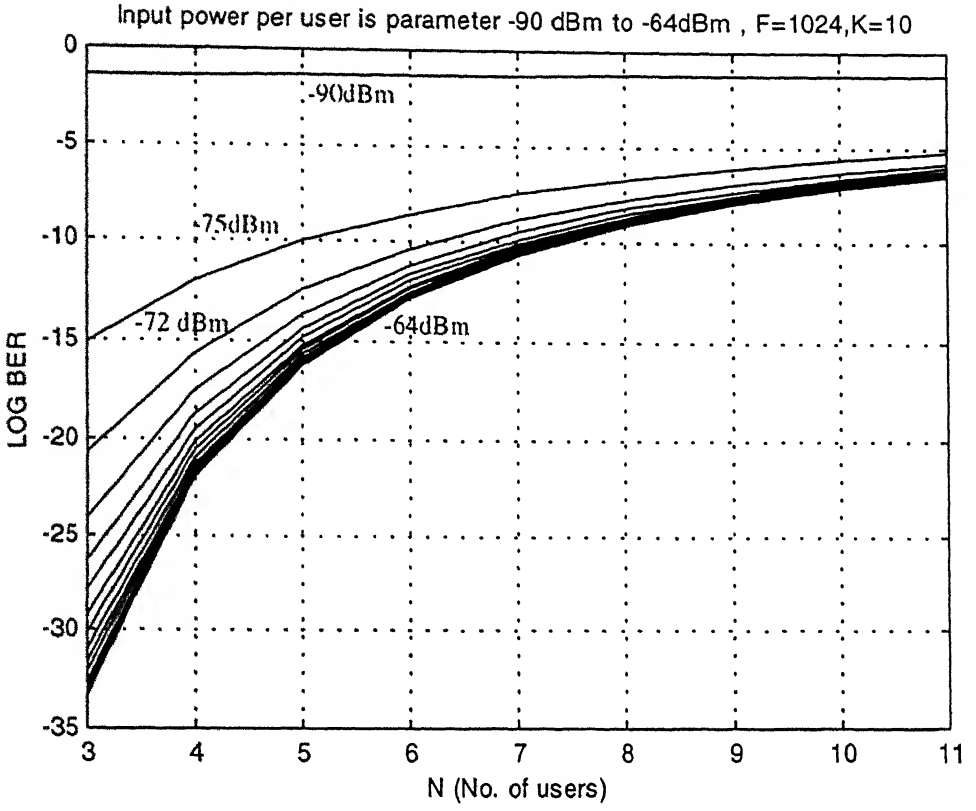

Figure 5.1.2 BER vs. number of users for low input power

The horizontal line at the top of Figure 5.1.2 shows that for very low power the performance is very poor. The medium power range is dominated by signal ASE noise, while the high power range is dominated by other user interference. In the high power region the performance does not change because in the other user interference region the interference signal is the property of code which decides BER. As the number of user increases, probability of interference increases, so the performance degrades.

A similar plot, with a larger code length, F=4096 is shown in Figure 5.1.3. The nature of the curves remains same, only the performance improves as compared to the previous case. We have varied N from 10 to 45 in this case. In the earlier case for N=10, BER $\approx 10^{-7}$, now for the same N, BER $\approx 10^{-30}$, which is a remarkable improvement. The worst BER in this case is also around 10^{-5}. The length of the code is limited by the bandwidth of fiber and other optical and electrical elements like amplifier, so it cannot be increased beyond a certain limit. If users are having signals of small bandwidth (which is not common in optical communication), then we can increase the code length to accommodate higher number of simultaneous users.

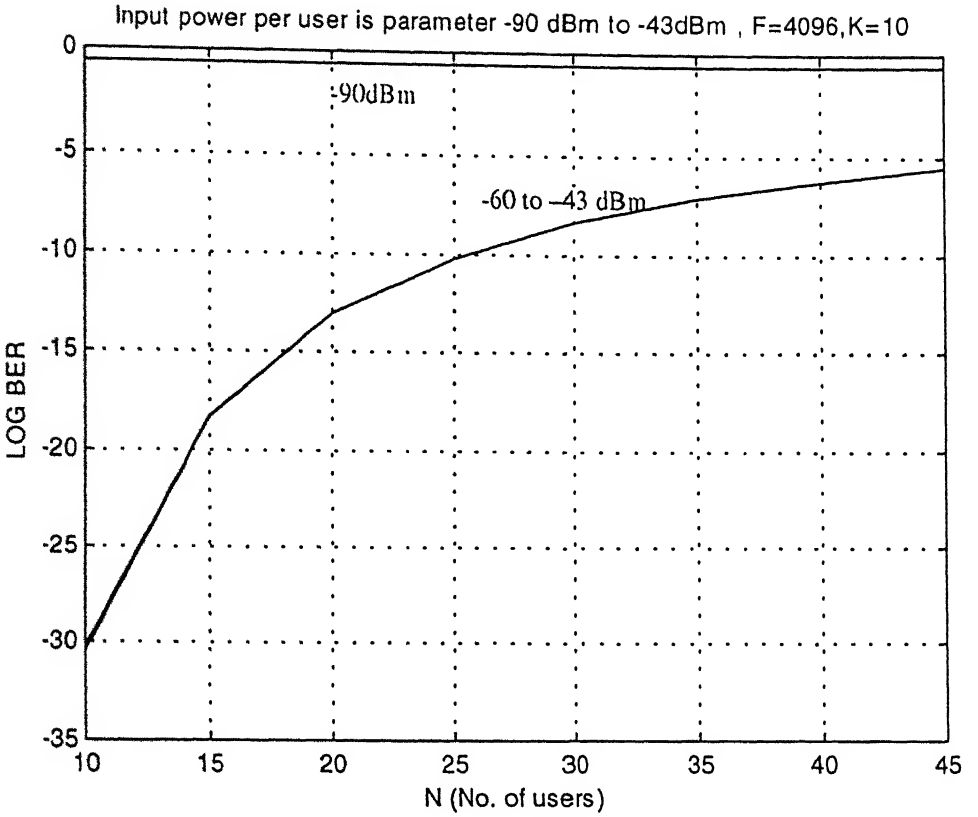

Figure 5.1.3 BER vs. number of users for a longer code length

5.2 BER VS. WEIGHT OF CODE

We have obtained BER variation with the weight of codes with two parameters: the number of users in the system and the input power to the receiver.

5.2.1 NUMBER OF USERS AS PARAMETER

The plot for the logarithm of BER vs. number of users in the OCDMA system, with number of users as a parameter is shown in Figure 5.2.1. We have used two values of length of code: 1024 and 4096. The input power is kept fixed at –40dBm. When the length of code is 1024, K is varied from 1 to 10, and N is varied from 3 to 11. We get different curves for different number of users in the system. These curves have the same nature-negative slope, showing that as the weight of code is increased for a given number of users, performance improves. This happens because as the code weight is increased the power of the desired signal increases, see Eqn. (4.3.4). For K=10, up to 9 simultaneous users can be accommodated with BER$\leq 10^{-10}$. Also as N increases the curves rise up, so the increase in the number of users deteriorates the system performance, as pointed out earlier also.

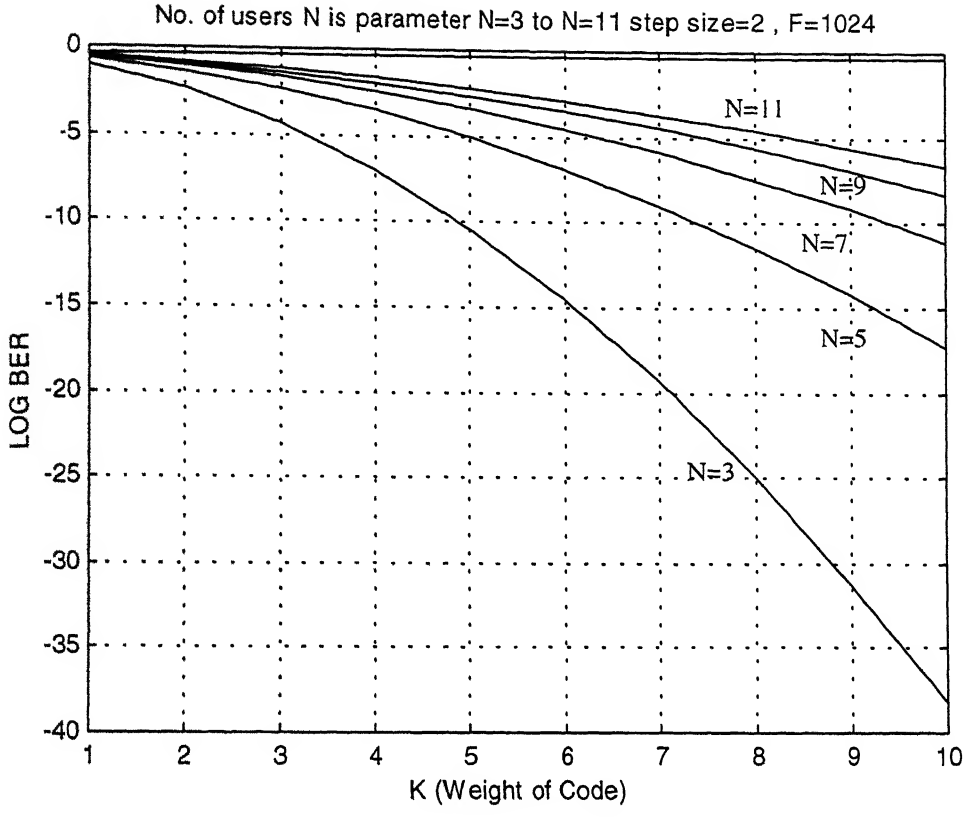

Figure 5.2.1 BER vs. Weight of code, number of users as parameter

The curves when plotted for F=4096, show a similar nature, see Figure (5.2.2). The performance improves a lot compared to the previous case. The number of users is varied from 10 to 46. So to achieve better performance either K can be increased, which automatically decreases the number of available OOCs for a given F, or F can be increased which in turn increases the number of available OOCs with the same K.

5.2.2 INPUT POWER AS PARAMETER

The plot of log of BER vs. weight of code, with input power as parameter is shown in Figure (5.2.3). For F=1024 and N=5, it is seen that for higher input power the performance of the system is independent of the input power. For BER$\leq 10^{-10}$, a code of weight 7 suffices.

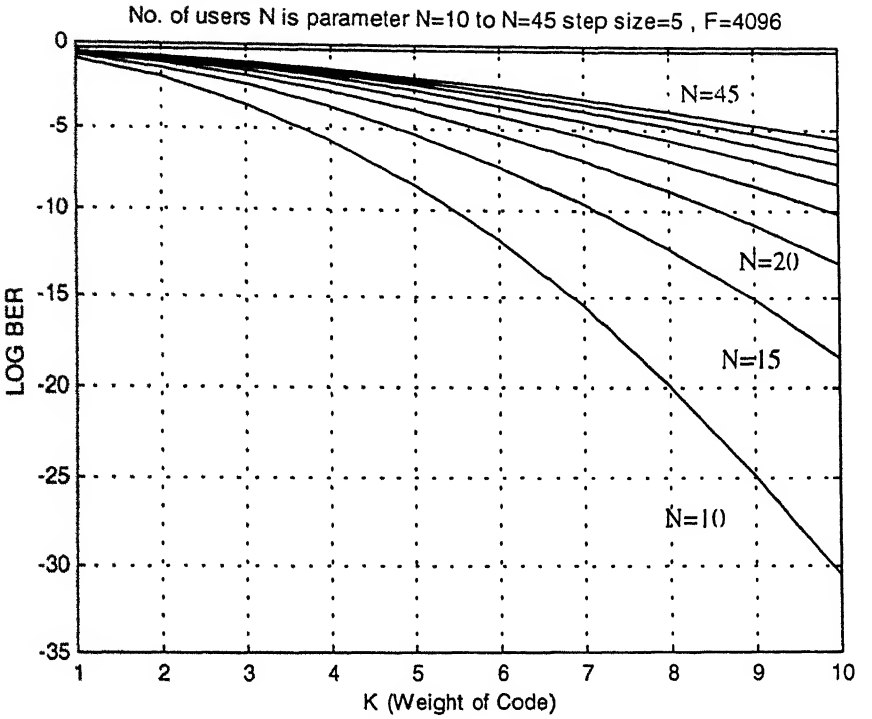

Figure 5.2.2 BER vs. Weight of code, number of users as parameter, larger code length

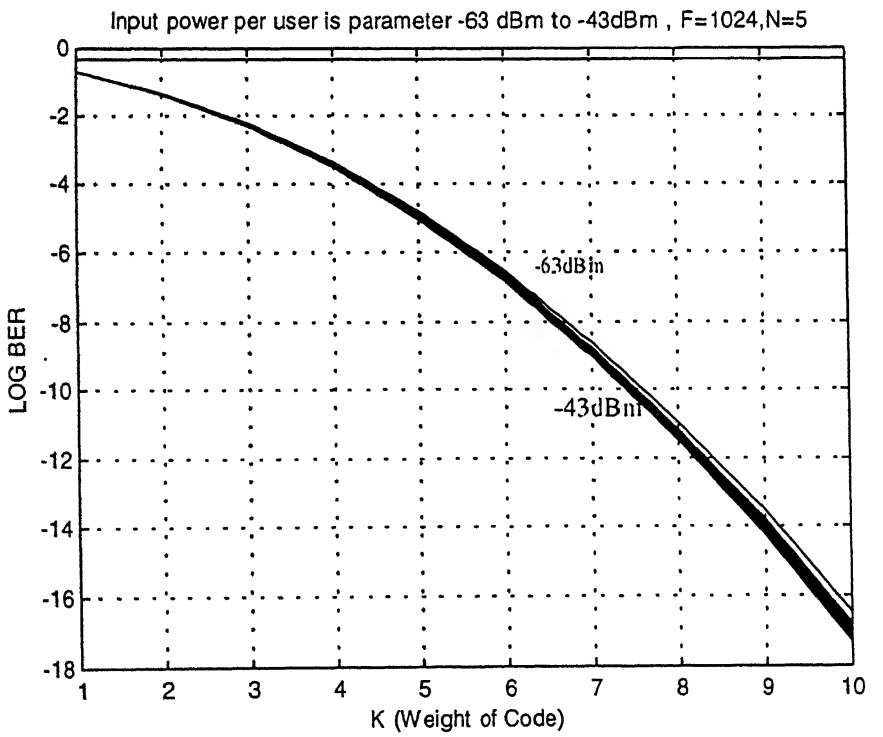

Figure 5.2.3 BER vs. weight of code, input power is parameter, high power range

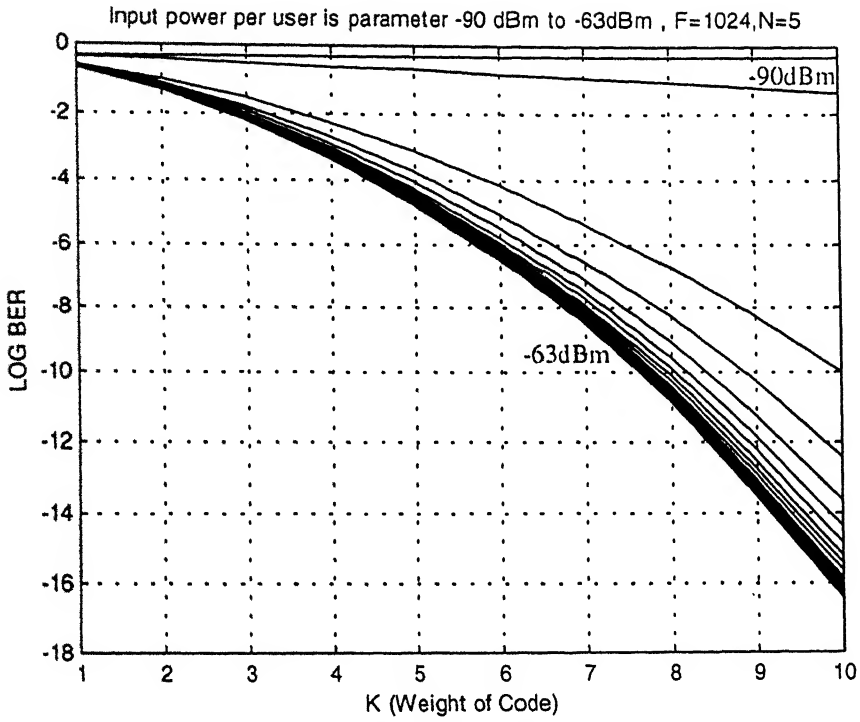

Figure 5.2.4 BER vs. Weight of code, input power is parameter, low power range

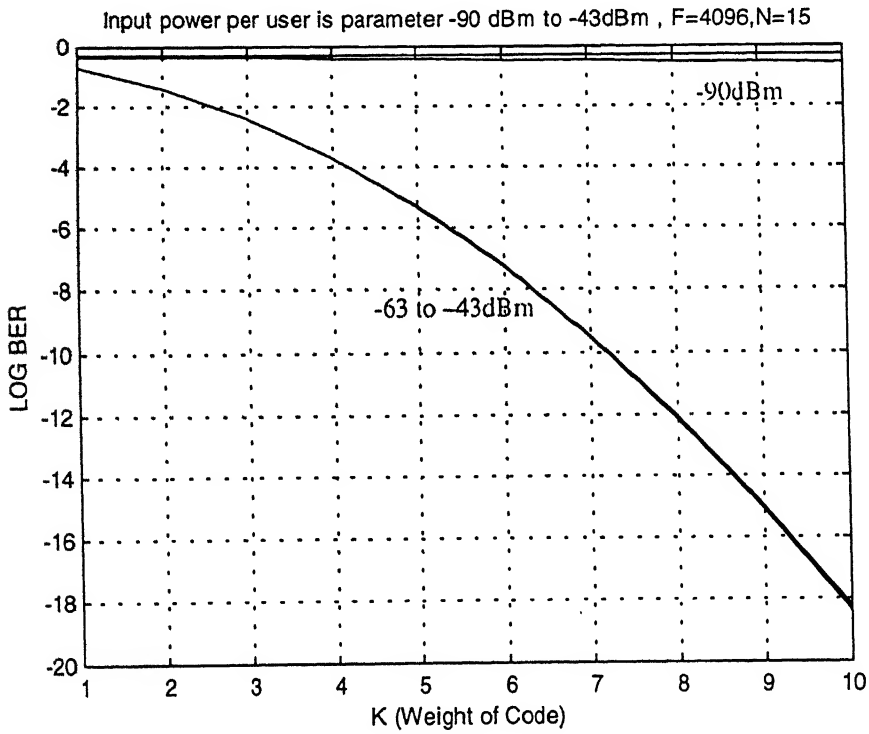

Figure 5.2.5 BER vs. Weight of code, longer code length,F=4096

The performance improves nearly linearly on log BER curve as weight of the code is increased. For a very low power values<-80dBm, we get a straight line in the graph at the top. The curve for the same variables is plotted for the low power values in Figure 5.2.4. This graph shows the transition from the poor BER to good values as input power is increased

For F=4096, and N=15, we have the results in Figure 5.2.5. These curves show that the performance improves as the code length is increased. Thus, for accommodating higher number of users, one should increase the length of the code; this as stated earlier increases the number of available OOCs.

5.3 BER VS. INPUT POWER

We have plotted it for two parameters, namely weight of the code and the number of users in the system.

5.3.1 WEIGHT OF CODE AS PARAMETER

The weight of code is varied for both F=1024 and F=4096. For F=1024 and N=5, see Figure 5.3.1, the curves show two distinct regions. The weight of code is varied from 1 to 9. For low power (<-60dBm), the curves have a negative steep slope, signal-ASE beat noise is the dominating source of noise in this region. In the zone where power is high the curves reach a floor for all values of weight of code although the saturated value of BER is different for different weights. This region has other user interference as the dominant source of noise. For higher K the performance is better than the lower K in high power region. On the contrary, in the low power region lower weight has better performance. This is the cause of crossover of the curves.

For F=4096, N=15, the nature of curves is same as that for previous case. The BER performance improves in this case as shown in Figure 5.3.2. We can say this because the BER in this case is nearly same as in the previous case, but as we have plotted it for 15 users (earlier there were only 5 users).

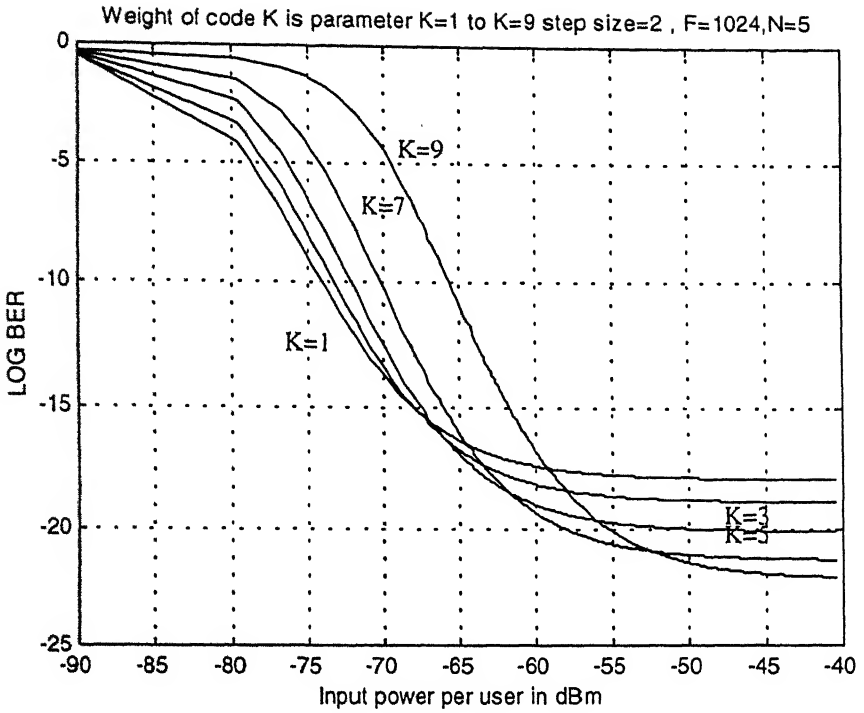

Figure 5.3.1 BER vs. input power, weight of code is parameter, F=1024

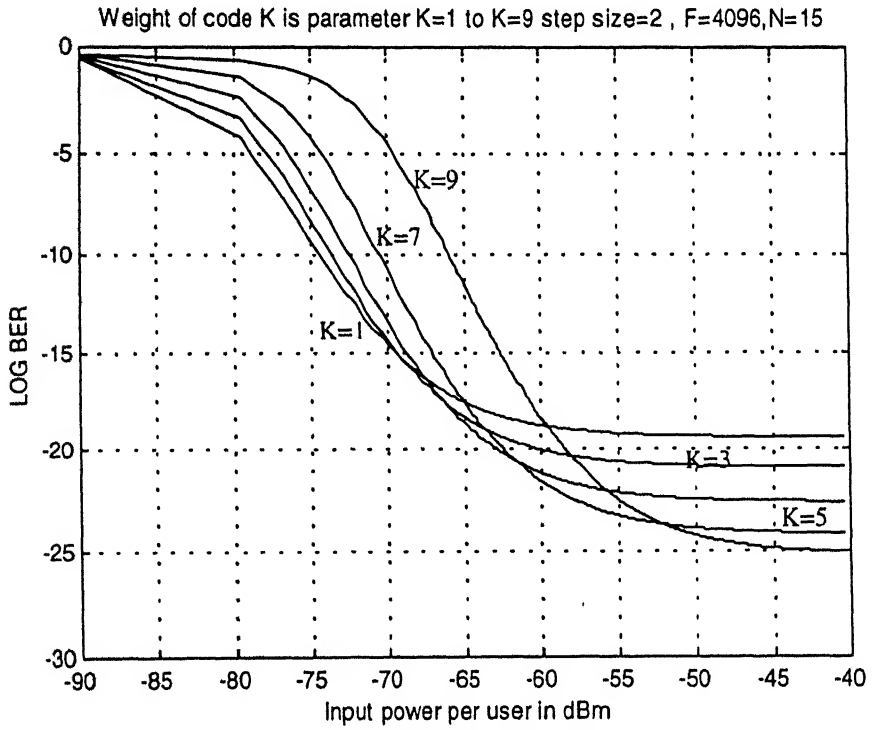

Figure 5.3.2 BER vs. input power, weight of code as parameter, F=4096

5.3.2 NUMBER OF USERS AS PARAMETER

For this we have plotted the results, both for F=1024 and F=4096. In Figure 5.3.3, for F=1024 and K=4, N is varied from 2 to 11, the curves have three distinct regions. At a very low input power (-90 to –80dBm), the curves have a small negative slope and for different values of N, the performance improves with increase in power. In this region both thermal and signal-ASE beat term is the dominant source of noise. At medium power input (-80 to –60dBm), the curves have a higher value of negative slope. The lower the value of N better is the performance, showing that in a system with less interferers the performance is better. In this region signal-ASE beat noise dominates over other noise terms. At large input power values the curves reach a floor, and there is no further improvement in BER. The saturation value of BER is greater for greater N. This region is governed by other users' interference noise.

For F=4096, K=4, the nature of curves is same as above, except that BER has improved as compared to the previous case, see Figure 5.3.4. This shows that the BER improves when the length of the code is increased.

5.4 SUMMARY OF RESULTS

We have plotted the variation of BER, with weight of OOC, number of simultaneous users in OCDMA system, and input power per user to the receiver as variables. For any two variables we have taken the third variable as a parameter, and each curve is drawn for two lengths of code: F=1024 and F=4096. The BER improves when the input power is increased. If the input power per user is greater than –60dBm, then the interference from other users is dominant source of noise. As the receiver sensitivity has typical value of –32dBm, therefore if we take 0.5dB/Km as attenuation by the fiber, we have achieved an increase of 56 Km in fiber span. Therefore if input power is 1mW then an OCDMA system with span of 100Km can be designed.

The performance also improves if the weight of the code is increased. We can accommodate 7 users such that BER<10^{-10}, with weight of code=10 and F=1024. If the weight of the code is 4, then less than 3 users can be accommodated with same parameter values [Figure 5.2.1].

If the number of users in the system is increased then the performance degrades. For –60dBm input power per user, F=1024, number of users with BER 10^{-23} is 4. For 7 users the BER is 10^{-10} [Figure 5.1.1].

As the length of code is increased the performance improves. For F=1024, K=10, and N=10, BER is 10^{-7}, while for other parameters kept same and F changed to 4096, BER is 10^{-30}. Thus, there is a drastic improvement in performance by quadrupling the length of code.

In the next chapter we will conclude our work.

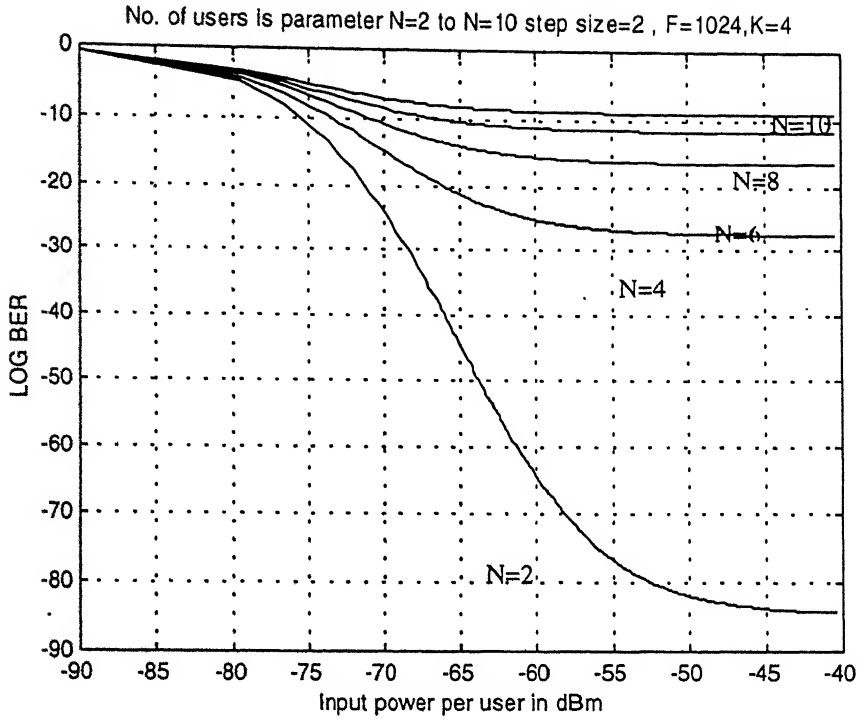

Figure 5.3.3 BER vs. Input power, number of user as parameter, F=1024

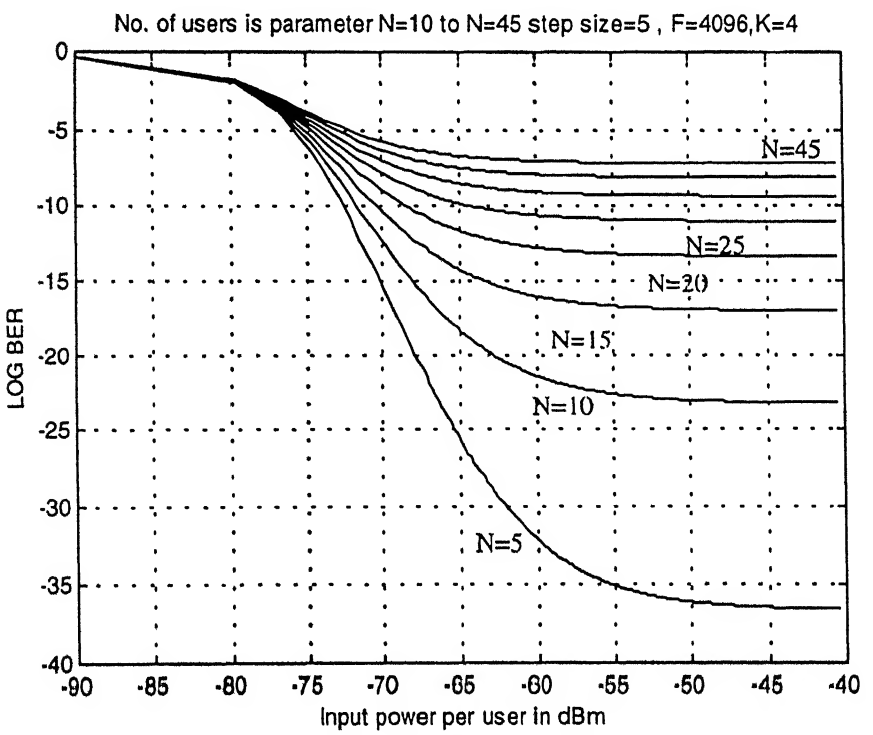

Figure 5.3.4 BER vs. Input power, number of users as parameter, F=4096

CHAPTER 6

CONCLUSION

In this work link analysis of optical CDMA (OCDMA) system has been done with optical preamplifier at the receiver end. The performance of such a system is affected by the weight of optical orthogonal code (OOC) used, length of OOC, number of users in the system, and input power per user at the receiver end. The effect of these factors on BER has been plotted using the expression we have got through analysis.

6.1 CONCLUSIONS

The following conclusions can be drawn from the results shown in the previous chapter:

1. As the number of users in the system increases the system performance degrades. This is an expected result because as the number of users increases, the interference signal from other users at the receiver of a particular user increases. This results in higher noise, which increases BER. The number of simultaneous users, which can be accommodated, with a code length of 4096, is 25 for BER $<10^{-10}$ [Figure 5.1.3]. The number of simultaneous users for code length of 1024 is 7 for the same BER requirement [Figure 5.1.1].

2. As the weight of OOC is increased the system performance improves in the region where the performance is governed by the other user interference as the dominant source of noise. This is observed for medium and higher input power at the receiver. This happens because on increasing the weight of code, the desired signal power increases, decreasing the BER. So using a high weight code yields a better performance, but this happens at the cost of decrease in the number of simultaneous users in the system, because the number of OOCs in a family is bounded and this bound is inversely proportional to the square of weight of code. For weight of code=7, 15 simultaneous users can be accommodated for BER$<10^{-10}$[Figure 5.2.2].

   At very low input power (<-80dBm), the signal-ASE beat noise is the dominant source of noise, and in this region the performance deteriorates with increase in the weight of code. But the BER value is very high and so the OCDMA system has to be operated in the medium to high power region [Figure 5.3.1 and 5.3.2].

3. The BER improves as the input power to the receiver is increased. At lower input power (<-80dBm) the performance is poorer but is independent of the small increase in power. At the medium power range (between –80 to –60dBm) the performance improves and desirable values of BER are achieved. At higher power values (>60dBm) the BER curve gets saturated and is independent of large increase in the power values. This saturation value depends on the weight of the code used and the number of users in the system [Figure 5.3.1 to 5.3.4].

   The typical value of sensitivity of PIN diode is –32dBm. It is observed in Figure 5.3.1 to 5.3.4 that for an input power per user to the receiver greater than –60dBm, system can be operated to work for BER $<10^{-10}$. Therefore in comparison to a system in which there is no preamplifier we can tolerate a link loss of 28dB. Assuming negligible splice losses, and fiber with 0.5dB/Km. attenuation, we can have an additional span of 56Kms. This is a remarkable improvement in the overall system.

4. We have drawn two sets of curves for two different values of length of code. The set of curves with F=4096 shows better performance than the set of curves with F=1024.So as the length of the OOC is increased the performance improves. This happens because for a given weight of code, if length is increased the probability of interference reduces resulting in reduced value of interference noise so BER decreases. The length of OOC is constrained by the bandwidth of the fiber and more tightly by the bandwidth of optical signal processing elements. If the user data rate is low then greater length codes can be used to achieve better performance.

These conclusions agree with the previous work [11]. We can see from Eqn.(2.2.1) that the SNR is proportional to the square of the length of code and inversely proportional to the number of users in the system. This is also concluded in points 1 and 2 above. The experimental value of BER without the use of optical preamplifier [11] for weight of code=10 and 10 users is 10^{-7}. In our system, for the same parameters BER$\approx 10^{-8}$. This shows that there is a slight improvement in performance. Thus we have increased the range of system without suffering degradation in performance.

On the basis of above conclusions we can design an OCDMA system with users having a data rate of 155Mbps. The OOC with code length=1024, weight=10 can be used for incorporating upto7 simultaneous users with BER$<10^{-10}$. If we increase the code length to 4096, then for the same performance 25 simultaneous can be incorporated. The fiber span can be up to 100Kms. The total number of users in the system can be larger than the simultaneous users.

6.2 SCOPE FOR FUTURE WORK

We have placed the optical amplifier after the matched filter in our analysis. It is interesting to analyze a system with the amplifier placed before the matched filter and compare its performance with our system.

The optical orthogonal codes, which we have used for the analysis, are the general codes given by Salehi [1]. The performance analysis of system with other OOCs such as Prime codes and Projective geometry codes can be done. A comparison can be done to judge the most suitable code for this purpose.

As described in [2], the system performance can be improved by reducing the effect of the interference signal intensity. For this a non-linear device can be incorporated before the optical tapped delay line (matched filter). An optical hard limiter is a device to clip the optical intensity, due to analog summation of the intensity of the interference signals during chip duration, to the value of the intensity due to the desired signal during that chip duration. Thus, the chance of crosscorrelation peaks achieving a value higher than autocorrelation peak at the matched filter output is nullified. This results in decreasing BER. A system analysis with such non-linear device can be done to see the improvement in performance in comparison to our system.

APPENDIX A

GAIN AND NOISE MODEL OF PHOTONIC AMPLIFIER

A.1 GAIN MODEL

The EDFA is modeled as a three level system. See Figure A.1.1.

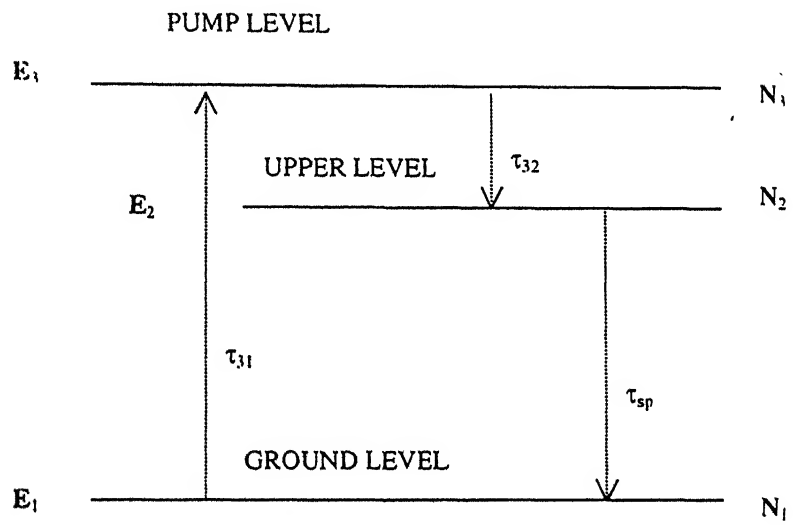

Figure A.1.1 Three Level Amplification

The silica core of fiber is doped with Er^{3+} ion, it is assumed that doped fiber is single mode at both pump and signal wavelength, so that all the parameters such as intensity, population density of each level are independent of azimuthal co-ordinate φ. Let $N_1(r,z)$ and $N_2(r,z)$ be the population density of Er^{3+} ion in ground state and the upper level respectively. Here r represents the cylindrical radial co-ordinate and z is along the axis of fiber. Pumping takes Er^{3+} ion from the ground state E_1 to the pump level E_3, from which ions relax very rapidly to the upper amplifier level E_2. It is assumed that the level E_3 is unpopulated since the relaxation rate of level E_3 is very high.

$$N_1(r,z)+ N_2(r,z) = N_t(r,z) \qquad (A.1.1)$$

$N_t(r)$ is ion density of Er^{3+}

The rate of change of population of the ground level E_1 is

$$\frac{dN_1}{dt} = -\frac{\sigma_{pa} I_p N_1}{h\upsilon_p} - \frac{\sigma_{sa} I_s N_1}{h\upsilon_s} + \frac{\sigma_{se} I_s N_2}{h\upsilon_s} + \frac{N_2}{\tau_{sp}} \qquad \text{(A.1.2)}$$

Here $\sigma_{pa}, \sigma_{sa}, \sigma_{se}$ are cross-section of fiber for pump, stimulated absorption and stimulated emission respectively.

$$\text{Let } \eta_s = \frac{\sigma_{se}}{\sigma_{sa}}$$

At steady state $\frac{dN_1}{dt} = 0$ so we get

$$\frac{N_2(r,z)}{N_1(r,z)} = \frac{I^*_p + \frac{I^*_s}{(1+\eta_s)}}{1 + \frac{\eta_s}{(1+\eta_s)} I_s^*} \qquad \text{(A.1.3)}$$

where

$$I^*_s(r,z) = \frac{I_s(r,z)}{I_{s0}} \quad ; \quad I_{s0} = \frac{h\nu_s}{\sigma_{sa}\tau_{sp}(1+\eta_s)} \qquad \text{(A.1.4)}$$

$$I_p^*(r,z) = \frac{I_p(r,z)}{I_{p0}} \quad ; \quad I_{p0} = \frac{h\nu_p}{\sigma_{pa}\tau_{sp}} \qquad \text{(A.1.5)}$$

Using eqn. (A.1.1) and (A.1.3)

$$N_2(r,z) = \frac{I^*_p + \frac{I^*_s}{(1+\eta_s)}}{(1 + I^*_p + I^*_s)} N_t \qquad \text{(A.1.6)}$$

$$N_1(r,z) = \frac{1 + \frac{\eta_s}{(1+\eta_s)} I^*_s}{(1 + I^*_p + I^*_s)} N_t \qquad \text{(A.1.7)}$$

From eqn. (A.1.6) and (A1.7),

$$\eta_s N_2(r,z) - N_1(r,z) = \frac{(\eta_s I^*_p(r,z) - 1)}{(1 + I^*_p(r,z) + I^*_s(r,z))} N_t \qquad \text{(A,1.8)}$$

Hence for amplification at a particular value of (r,z), condition is

$$I^*_p(r,z) > \frac{1}{\eta_s} \text{ or } I_p(r,z) > I_{pt} = \frac{1}{\eta_s} I_{p0} \qquad \text{(A.1.9)}$$

Here I_{pt} is called threshold pump intensity. Thus a minimum pump intensity is needed at any value of (r,z) to achieve amplification.

A.2 ASE NOISE STATISTICS

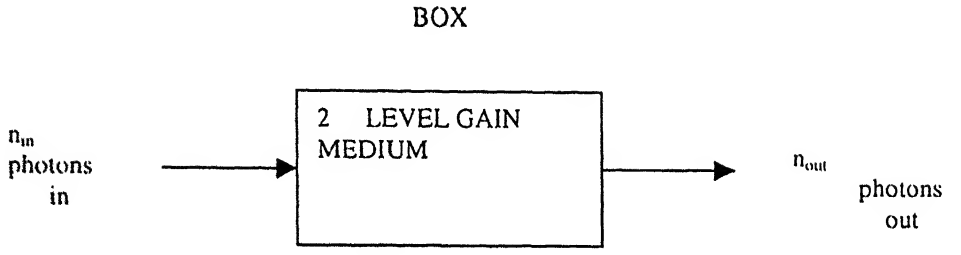

Figure A.2.1 Photon amplification in a gain medium

Consider a 2 level gain medium as shown in Figure A.2.1 in which at any time t, n (t) is the number of photons contained in the box.

Let Pr{n photons}=n(t)

As the photons are incident on the gain medium, stimulated and spontaneous emission occur accompanied by absorption. Due to these processes n(t) is varying - increasing due to emission and decreasing due to absorption.

Let the stimulated emission rate=a_1, spontaneous emission rate=a_2, and stimulated absorption rate=b.

$$a_1 = \sigma_{se} N_2$$
$$b = \sigma_{sa} N_1$$
$$a_2 = \frac{N_2}{\tau_{se}}$$

here σ_{sa}, σ_{se} are stimulated emission and stimulated absorption area of cross-section N_1, N_2 are the particle density in lower energy state (E_1) and higher energy state(E_2) respectively.
τ_{se} is stimulated emission time constant.

Assume $a_1=a_2=a$ and $a > b$
The state diagram of system is shown in Figure A.2.2.

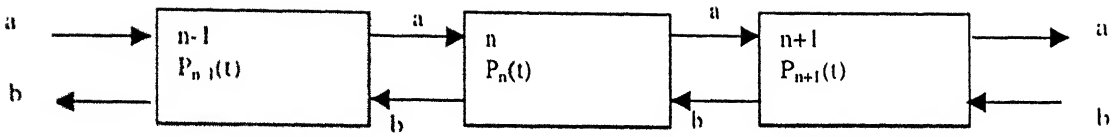

Figure A.2.2 State diagram of number of photons in the system

where the state represents the number of photons in the system which increments by one by an emission and decrements by 1 by an absorption.

Prob. of system staying in state in state n=-[Prob. of system going out of state n]+[Prob. of system coming in state n]

$$\frac{dP_n(t)}{dt} = -[bn + an + a]P_n(t) + a(n-1)P_{n-1}(t) + b(n+1)P_{n+1}(t) + aP_{n-1}(t) \quad \text{(A.2.1)}$$

The last term is due to spontaneous emission from state n, which is independent of the number of photons in this state.

Under steady state, i.e., $\frac{dn}{dt} = 0$

$$\frac{d\langle n(t)\rangle}{dt} = (a-b)\langle n(t)\rangle + a \quad \text{(A.2.2)}$$

$$\frac{d\langle n^2(t)\rangle}{dt} = 2(a-b)\langle n^2(t)\rangle + (3a+b)\langle n(t)\rangle + a \quad \text{(A.2.3)}$$

$\langle\ \rangle$ denotes average over n

Using initial condition

$$\langle n(t)\rangle|_{t=0} = \langle n_0\rangle \quad \text{(A.2.4)}$$

Eqn. (A.2.2) reduces to

$$\langle n(t)\rangle = \langle n_0\rangle e^{(a-b)t} + \frac{a}{a-b}[e^{(a-b)t} - 1] \quad \text{(A.2.5)}$$

It is clear that for achieving gain with passage of time we should have $a > b$

After some time $T \approx \frac{Ln_r}{c}$ where L is length of gain medium and n_r is refractive index of medium we have

$$\langle n(T)\rangle = \langle n_0\rangle e^{(a-b)T} + \frac{a}{a-b}[e^{(a-b)T} - 1] \qquad \text{(A.2.6)}$$

Here $e^{(a-b)T}$ is one pass gain =G

So $$\langle n_{out}\rangle = G\langle n_{in}\rangle + \frac{a}{a-b}(G-1) \qquad \text{(A.2.7)}$$

Since a and b are proportional to N_2 and N_1 respectively

$\therefore n_{sp} = \frac{a}{a-b} = \frac{N_2}{N_2 - N_1}$ is defined as spontaneous emission factor.

Similarly solving (A.2.3) for $\langle n^2(t)\rangle$, if variance of n(t) is $\sigma^2(t)$ then

$$\sigma^2(t)\,|_{t=T} = \langle n_{in}\rangle e^{(a-b)T} + n_{sp}[e^{(a-b)T} - 1] + 2n_{sp}[e^{(a-b)T} - 1]\langle n_{in}\rangle e^{(a-b)T} + n^2{}_{sp}[e^{(a-b)T} - 1]^2 + e^{2(a-b)T}[\langle n^2{}_{in}\rangle - \langle n_{in}\rangle^2 - \langle n_{in}\rangle] \qquad \text{(A.2.8)}$$

Or

$$\sigma^2{}_{out} = \langle n_{in}\rangle G + n_{sp}(G-1) + 2n_{sp}(G-1)G\langle n_{in}\rangle + n^2{}_{sp}(G-1)^2 + G^2[\langle n^2{}_{in}\rangle - \langle n_{in}\rangle^2 - \langle n_{in}\rangle] \qquad \text{(A.2.9)}$$

In the eqn. (A.2.9) first term is amplified mean input photon number; second term is ASE noise; third term is product of signal and ASE; fourth term is product of ASE with itself; fifth term can be written as,

$$G^2[\sigma^2{}_{in} - \langle n_{in}\rangle] \qquad \text{(A.2.10)}$$

If the photon arrival distribution is Poisson, then this term is nullified (for Poisson distribution mean=variance), and so this term is called amplified deviation from Poisson.

APPENDIX B

PROBABILITY DENSITY FUNCTION FOR INTERFERENCE SIGNAL

In OCDMA system the correlated output of the signal of the other users with the code of desired user is the interference signal for the desired user. The output of the equivalent matched filter is a random variable. The exact evaluation of probability density function for I_1, the interference signal for the user 1, will require the knowledge of pdf associated with each $I_n^{(1)}$, for $2 \leq n \leq N$, since there are N users in the FO-CDMA system. The interference I_j at the output of the j^{th} receiver contains (N-1) interference terms so a total knowledge of N(N-1)/2 pdfs would be required. This task is lengthy and tedious for large N. Therefore two extreme cases for the analysis of interfering signals are chosen to make the calculations on probability density and associated BER mathematically more convenient.

1. Chip synchronous

In this case it is assumed that during crosscorrelation process the two signature sequences are shifted by a multiple of chip length while correlating. So shift is a discrete variable. Hence the correlation outputs are integral quantities (as partial overlap is restricted). This imposes upper bound on BER.

2. Chip asynchronous

In this case the correlation process can involve fractional chip interval shift of the sequences (i.e. shift as a continuous variable). This imposes lower bound on BER.

So BER (case 1) $\leq$ BER(exact) $\leq$ BER(case2)

B.1 INTERFERENCE DUE TO ANY ONE INTERFERER ON USER 1

The interference signal is composed of (N-1) interference signals arriving at the receiver of user 1.The intensity of interference optical signal on the receiver 1 due to anyone of the (N-1) interferers (say user n) is given by

$$I_n^{(1)} = \frac{W_n}{T_c}\int_0^{\tau_n} DP_n(t-\tau_n)b_n(t-\tau_n)DP_1(t)dt + \frac{W_n}{T_c}\int_0^{\tau_n} DP_n(t-\tau_n)b_n(t-\tau_n)DP_1(t)dt \qquad (B.1)$$

where

W_n is the n[th] user's received optical intensity at the user 1 receiver

τ_n is the delay of the n[th] user signal at the user 1 receiver, it is a random variable with uniform distribution on the interval (0,T)

$b_n(t)$ is the binary data signal of the n[th] user

$DP_n(t)$ is OOC for nth user

T_c is the chip duration of the code (signature)

From (4.2.2) it can be written

$$b_n(t-\tau_n)=\begin{cases} b_{-1}^{(n)} for 0 \le t \ge \tau_n \\ b_0^{(n)} for \tau_n \le t \ge T \end{cases} \qquad \text{(B.2)}$$

T is one bit duration of user data

Further τ_n can be expressed as the sum of two random variables M_n and $\rho_n . M_n$ is a random variable, which can take on any integer value in the interval [0,F-1] with equal probability. ρ_n is a random variable, which is uniformly distributed in the interval (0,1) i.e.

$$\tau_n = (M_n + \rho_n)T_c \qquad \text{(B.3)}$$

τ_n of (B.2) is defined as the epoch time associated with the n[th] user, and it represents the chip misalignment time between the locally generated OOC and the n[th] user. The two cases discussed above are analyzed separately.

1. Chip synchronous

In this case $I_n^{(1)}$ can be written as

$$\frac{I_n^{(1)}}{W_n} = b_{-1}^{(n)} \sum_{j=0}^{M_n-1} A_j^{(1)} A^{(n)}{}_{F-M_n} + b_0^{(n)} \sum_{j=M_n}^{F-1} A_j^{(1)} A^{(n)}{}_{j-M_n} \qquad \text{(B.4)}$$

The random variable $\frac{I_n^{(1)}}{W_n}$ can take two values, 0 or 1(this is due to crosscorrelation property of the two OOCs with λ_c=1*)

$$\text{Let } p = \Pr\left\{\frac{I_1^{(n)}}{W_n} = 1\right\} \qquad \text{then } \Pr\left\{\frac{I_1^{(n)}}{W_n} = 0\right\} = 1 - p = q \qquad \text{(B.5)}$$

So the probability distribution for the above random variable $\frac{I_n^{(1)}}{W_n}$ can be expressed as

---

* See Section 2.1.1

$$P_{\frac{I_n^{(1)}}{W_n}}\left(\frac{I_n^{(1)}}{W_n}\right)=q\delta\left(\frac{I_n^{(1)}}{W_n}\right)+p\delta\left(\frac{I_n^{(1)}}{W_n}-1\right) \tag{B.6}$$

From (B.6)

$$E\left\{\frac{I_n^{(1)}}{W_n}\right\}=p \qquad ; \qquad \text{E denotes expectation} \tag{B.7}$$

If $b_0^{(1)}, b_{-1}^{(n)}$, and M_n are independent random variables then from eqn. (B.2)

$$E\left\{\frac{I_n^{(1)}}{W_n}\right\}=p=\frac{K^2}{2F}$$

Putting value of p in (B.6)

$$P_{\frac{I_n^{(1)}}{W_n}}\left(\frac{I_n^{(1)}}{W_n}\right)=\left(1-\frac{K^2}{2F}\right)\delta\left(\frac{I_n^{(1)}}{W_n}\right)+\frac{K^2}{2F}\delta\left(\frac{I_n^{(1)}}{W_n}-1\right) \tag{B.8}$$

So

$$E\left\{I_n^{(1)}\right\}=W_n\frac{K^2}{2F} \tag{B.9}$$

and

$$\text{var}\left(I_n^{(1)}\right)=W^2{}_n\ \text{var}\left(\frac{I_n}{W_n}\right)=W_n{}^2\left(1-\frac{K^2}{2F}\right)\frac{K^2}{2F} \tag{B.10}$$

2. CHIP ASYNCHRONOUS

Replacing (B.2) and (B.3) into (B.1) and carrying out the integration, $I_n^{(1)}$ can be expressed as

$$\begin{aligned} I_n^{(1)} &= b_{-1}^{(n)}\left[\rho_n\sum_{j=0}^{M_n}A_j^{(1)}A^{(n)}{}_{F-M_n-1+j}+(1-\rho_n)\sum_{j=0}^{M_n-1}A_j^{(1)}A^{(n)}{}_{F-M_n+j}\right] \\ &+ b_0^{(n)}\left[\rho_n\sum_{j=M_n+1}^{F-1}A_j^{(1)}A^{(n)}{}_{j-M_n-1}+(1-\rho_n)\sum_{j=M_n}^{F-1}A_j^{(1)}A^{(n)}{}_{j-M_n}\right] \end{aligned} \tag{B.11}$$

In general the pdf for the above chip asynchronous signal can be given as [1]

$$P_{I_n^{(1)}}(I_n^{(1)})=q\delta(I_n^{(1)})+(1-q)\left|I_n^{(1)}\right| \tag{B.12}$$

where

$$|x| = \begin{cases} 1 for 0 \le x \ge 1 \\ 0 elsewhere \end{cases}$$

From [1] we have

$$E\{I_n^{(1)}\} = 1 - \frac{q}{2} = W_n \frac{K^2}{F} \quad \text{(B.13)}$$

and

$$\text{var}(I_n^{(1)}) = W_n^2 \, \text{var}(I_n^{(1)}) = W_n^2 (1-q)\left(\frac{1}{3} - \frac{1-q}{4}\right) = W_n^2 \left[\frac{2K^2}{F}\left(\frac{1}{3} - \frac{K^2}{2F}\right)\right] \quad \text{(B.14)}$$

B.2 INTERFERENCE DUE TO ALL INTERFERERS ON USER 1

As the number of interferers (N-1) is large, and the interfering signals due to each of them are independent random variables, so central limit theorem can be invoked. The resultant signal has Gaussian distribution, whose mean and variance are the sum of the mean and variance of the individual interfering signal distributions respectively.

If the net interference on user 1 is denoted by $I = \sum_{n=2}^{N} I_n$ then,

$$E\{I_1\} = E\left\{\sum_{n=2}^{N} I_n^{(1)}\right\} = \begin{cases} (N-1)\frac{K^2}{2F} W_n for, chip - syn. \\ (N-1)\frac{K^2}{F} W_n for, chip - asyn. \end{cases} \quad \text{(B.15)}$$

$$\text{var}(I_1) = \text{var}\left(\sum_{n=2}^{N} I_n^{(1)}\right) = \begin{cases} W_n^2 (N-1)\frac{K^2}{2F}\left(1 - \frac{K^2}{2F}\right) for, chip - syn. \\ W_n^2 (N-1)\frac{2K^2}{F}\left(\frac{1}{3} - \frac{K^2}{2F}\right) for, chip - asyn. \end{cases} \quad \text{(B.16)}$$

LIST OF REFERENCES

1. J.A. Salehi, "Code Division Multiple-Access Techniques in Optical Fiber Networks-Part I : Fundamental Principles", IEEE Transactions on Communications, Vol. 37, No. 8, August 1989.

2. J.A. Salehi and C.A. Brackett, "Code Division Multiple-Access Techniques in Optical Fiber Networks-Part II : System Performance Analysis", IEEE Transactions on Communications, Vol. 37, No. 8, August 1989.

3. J.A. Salehi, "Emerging Optical Code-Division Multiple Access Communication Systems", IEEE Network 1989.

4. F.R.K. Chung, J.A. Salehi, V.K. Wei, "Optical Orthogonal Codes: Design, Analysis, and Applications", IEEE Transactions on Information Theory, Vol. 35, No.3, May 1989.

5. M. Choudhary, P.K. Chatterjee, and J. John, "Code Sequences for Fiber Optic CDMA Systems", Dept. of Electrical Eng., IIT Kanpur.

6. A.S. Holmes and R.A. Syms, "All Optical CDMA Using Quasi Prime Codes", Journal of Lightwave Technology, Vol. 10, No.2, February 1992.

7. S.V. Maric, Z.I. Kostic, and E.L. Titlebaum, "A New Family of Optical Code Sequences for Use in Spread -Spectrum Fiber-Optic Local Area Networks", IEEE Transactions on Communications, Vol. 41, No. 8, August 1993.

8. W.C. Kwong, P.A. Perrier, and P.R. Prucnal, "Performance Comparison of Asynchronous and Synchronous Code Division Multiple Access Techniques for Fiber-Optic Local Area Networks", IEEE Transactions on Communications, Vol. 39, No. 11, November 1991.

9. N.A. Olsson, "Lightwave Systems with Optical Amplifiers", Journal of Lightwave Technology, Vol. 7, No. 7, 1989.

10. C.R. Giles, E. Desurvire, "Propagation of Signal and Noise in Concatenated Erbium-Doped Fiber Optical Amplifier", Journal of Lightwave Technology, Vol. 9, No. 2, February 1991.

11. P.R. Prucnal, M.A. Santoro, "Spread Spectrum Optic Local Area Network Using Optical Processing", Journal of Lightwave Technology, Vol. 4, No. 5, May 1986.

12. E. Marom,"Optical Delay Line Matched Filters" IEEE Transactions on Circuits and Systems, Vol. 25, No. 6, June 1978.

13. G.P. Aggarwal, "Fiber Optic Communication System", John Wiley and Sons Pvt. Ltd., 1992.

14. R.M. Gagliardy and S. Karp, "Optical Communication", John Wiley and Sons, 1976.

15. P.E. Green, "Fiber Optic Networks", Prentice Hall, 1993.

16. A.M. Weiner, J.P. Heritage, and J.A. Salehi, "Encoding and Decoding of Femtosecond pulses", Optics Letters, Vol. 13, 1988.

17. A. Ghatak and K. Thyagarajan, "Introduction to Fiber Optics", Cambridge University Press, 1998.

A 130788

Date Slip

This book is to be returned on the date last stamped.